Transportation Research Part C 130 (2021) 103322

Contents lists available at ScienceDirect

Transportation Research Part C

journal homepage: www.elsevier.com/locate/trc

Design of an arterial signal progression plan for multi-path flows with only intersection turning counts

Yen-Hsiang Chen, Yao Cheng *, Gang-Len Chang

Department of Civil & Environmental Engineering, University of Maryland, College Park, USA

ARTICLE INFO

Keyword:
Multi-path progression
Local paths
Heavy turning flows
Mutual queue blockage

ABSTRACT

Most congested urban arterials, connecting multiple major intersections with heavy turning flows, are likely to comprise multiple high-volume path flows in addition to its through traffic. Hence, such arterials, if designed with state-of-the-art models for progressing mainly through traffic flows, cannot achieve the expected level of performance, because those heavy path flows involving turning movements will inevitably suffer from overflows at their turning bays and consequently trigger a mutual blockage between the turning and through traffic flows. Although some recent advances on multi-path signal progression (Yang et al., 2015; Arsava et al., 2016) offer a viable design alternative for arterials accommodating such traffic patterns, their required data such as the arterial's O-Ds or path volume information cannot be collected with state-of-the-practice traffic sensors, or mathematically estimated at the accuracy level sufficient for design of control strategies. As such, this study proposes a model with the optimized phase sequence and offsets to produce a progression band for each candidate path along the target arterial with only each intersection's volume counts, based on the set of "local bands" for all local paths constituted by each link's upstream flow-in and downstream flow-out movements. Such identified local progression bands are then optimally connected between two neighboring links to form the progression band for traffic flows on each path to progress over multiple arterial links under the objective of maximizing the total weighted progression bands. To ensure the effectiveness of the produced progression bands, the proposed model has accounted for all factors and geometric constraints that may cause their mutual impedance in design of the offsets and phase sequences. The results of extensive numerical experiments with respect to delay and the number of stops per vehicle (reduced by 5.8% and 9.9%, respectively, compared to the benchmark model) within the entire network have shown the effectiveness of the proposed model.

1. Introduction

Traffic flows on most urban arterials are often plagued by frequent stops, mutual queue blockage between turning and through vehicles, and excessively long delays for both through and turning movements. Aside from high intersection volumes, key contributors for such congestion typically include: queue spillback from the insufficient tuning-bay length, through queue formation on short links, and ineffective progression for either through or turning path flows. The popular design notion of providing two-way signal progression (Morgan and Little, 1964; Little, 1966; Messer et al., 1973; Little et al., 1981; Gartner et al., 1991; Papola, 1992; Chaudhary et al., 2002; Li, 2013; Zhang et al., 2015) by the traffic community for such arterials generally cannot adequately account for those

* Corresponding author at: University of Maryland, College Park, USA.

https://doi.org/10.1016/j.trc.2021.103322
Received 10 August 2020; Received in revised form 19 July 2021; Accepted 20 July 2021
Available online 5 August 2021

congestion contributors, and thus often suffers from insufficient progression bandwidth to accommodate non-through path flows. Fig. 1 shows such an example in North Bethesda, Maryland, where the arterial segment serves to connect a commuting freeway with the urban network. Those heavy turning flows to and exiting from I-270, not explicitly included in design of the arterial's signal progression plan, often produce overflows at the turning bays and result in excessive queues to impede the through lanes.

Most two-way arterial progression models, due to their focus on the through traffic flows, often cannot achieve the expected level of performance under the following multi-path traffic scenarios: 1) heavy turning-in and turning-out flows over each link are not provided with progression and thus may experience excessive delay and queues; and 2) the effectiveness of through progression is likely to be impeded by turning traffic queues. Recognizing such limitations, a recent study by Yang et al.(2015) indicates the need to provide multi-path progression bands for all primary path flows along the arterial (see Fig. 2(a)), including not only those for through movements but also vehicles taking turning movements at major intersections after traveling over consecutive arterial links. A study for the same purpose but with a different methodology by Arsava et al. (2016) presents the OD-BAND model that can produce the set of path-based progression bands, based on the given volume distribution over all traffic paths on the target arterial. Both studies concluded that with a designated progression band for each intersection's traffic stream taking different movements, the arterial is expected to experience much less delay, shorter queues, and smooth traffic conditions (Yang et al., 2015).

Development of such a multi-path progression model for effective use in practice, however, remains a very challenging task, because the information of volume distribution between different paths and potential interference between their designated progression bands is not available yet with existing arterial surveillance technologies. For example, as shown in point A in Fig. 3, overflows from a left-turn bay may reduce the available bandwidth designated for use by through progression flows. By the same token, the formation of excessive queues from through vehicles may also block the entry of flows to the left-turn lane, as shown at point B in

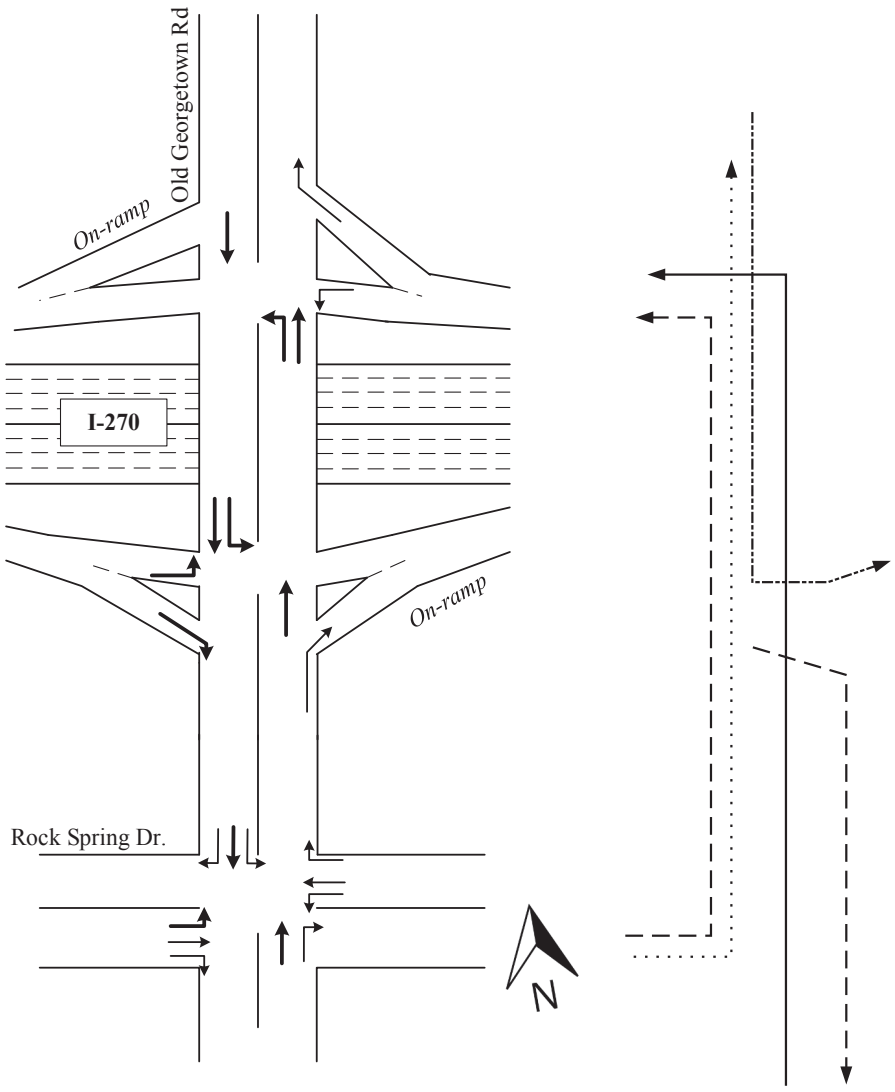

Fig. 1. An arterial segment with heavy turning counts and multi-path of traffic flows.

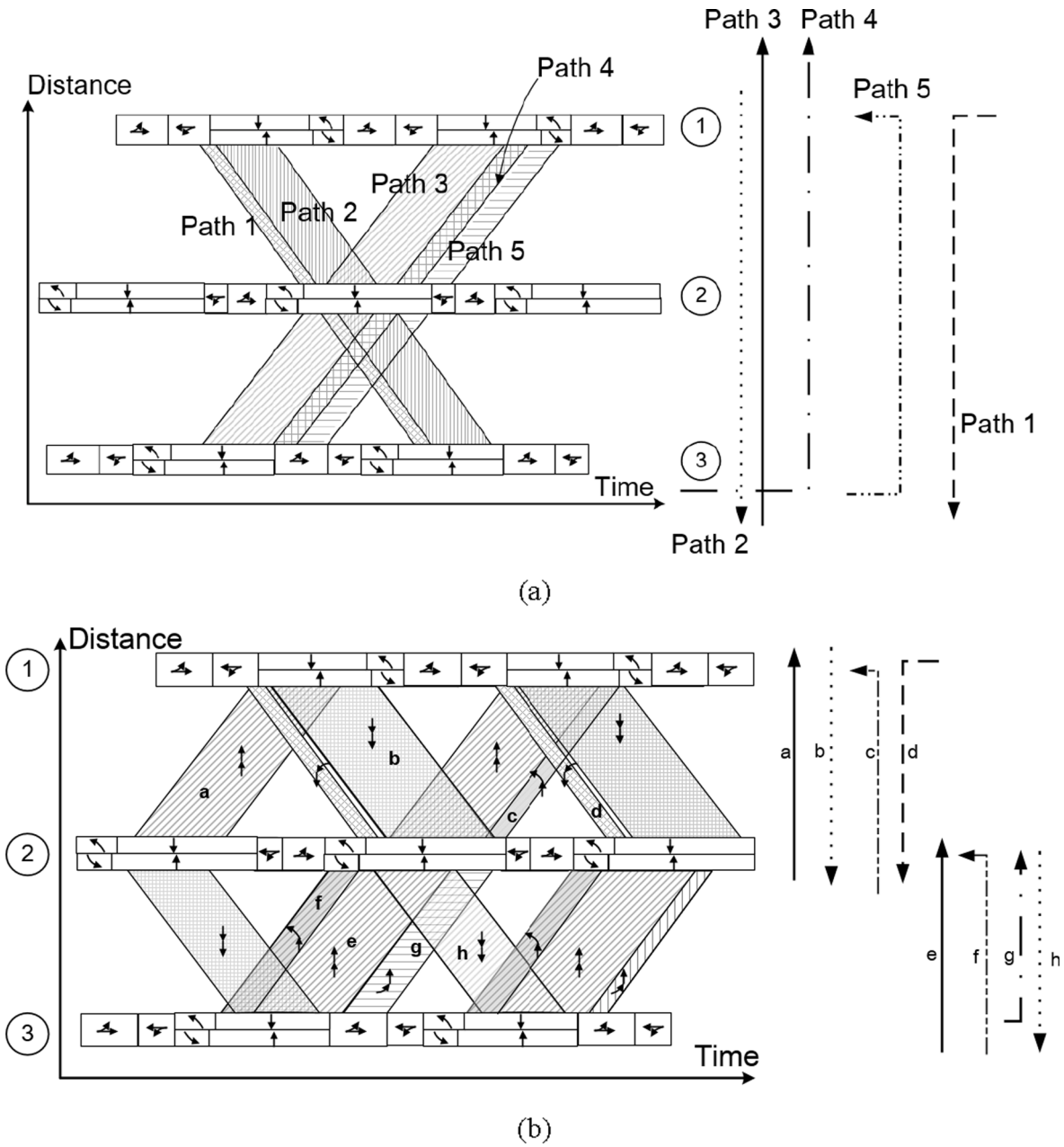

Fig. 2. Multiple-movement progression (a) by multi-path progression (Yang et al., 2015); (b) by local path progression.

Fig. 3. Such critical information that may impact the effectiveness of a multi-path arterial progression system is not available from field measurement. Likewise, the essential information of an arterial's traffic O-D and volume distribution for the path-based progression design cannot be directly measured with existing traffic monitoring sensors. Although deriving such information from the available intersection's turning volume counts is a viable alternative, producing such essential information at the level of accuracy and precision for signal control due to its highly under-determined nature remains a challenging ongoing research task for the traffic community (Yang and Chang, 2017).

Hence, for any signal progression model to be used effectively in practice for arterials accommodating multi-path traffic flows, it is desirable to have the following key features (1) relying only on readily available and reliable data (e.g., intersection turning volumes); (2) offering a progression band for each observable path of traffic flows having significant volume; and (3) preventing potential mutual blockages (see Fig. 3) between turning and through traffic queues to ensure the full utilization of each designated bandwidth. With such required features in mind and also to circumvent the difficulty of estimating an O-D volume table for the arterial, this study has addressed this vital subject from a different perspective, that is, to offer a link-based progression band, named local progression band

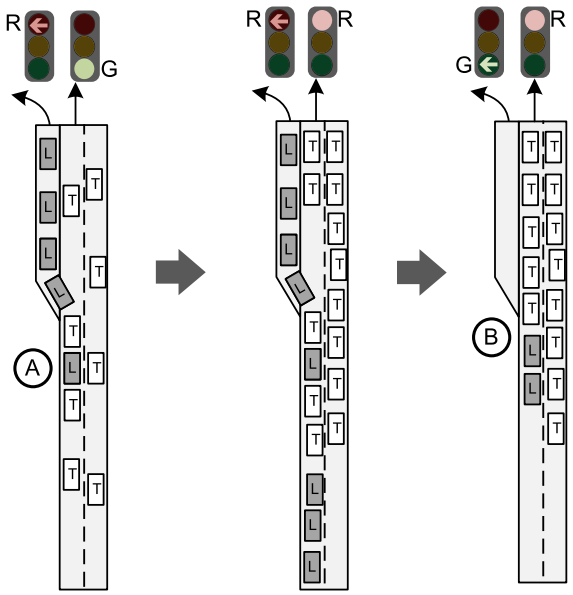

Fig. 3. Mutual blockage of left-turn and through vehicles.

(see Fig. 2(b)), for each traffic stream from entering to exiting a link via either the through or turning phase, and then connecting all such local bands between consecutive links to constitute the arterial's multi-path progression system.

More specifically, with the proposed modeling notion, one will first design the progression band for traffic flows along each local path, constituted by vehicles entering each link from its upstream intersection and moving out its downstream intersection during either the turning or through phase. Fig. 2(b) shows an example of such local progression bands for local path flows. By optimizing the connection between two neighboring links' local bands for through movement, one can then extend the local bands for various local traffic movements to establish the progression bands for multi-path flows over multiple links of the arterial without their O-D or path volume information. For example, the progression bands for path 5 (moving into the northbound link during the upstream left-turn phase and exiting the link via the downstream left-turn phase) in Fig. 2(a) can be constructed by connecting the local Path-c and Path-g in Fig. 2(b). Since each local path extends to only two neighboring intersections, one can apply readily available tuning volume counts to design the signal coordination for such local paths.

In review of the literature on arterial signal control, it is noticeable that most studies lie in either of the following two categories: delay minimization and progression bandwidth maximization. In the former category, TRANSYT, a simulation-based optimization model, is one of the most established tools in practice for the design of signal plans (Robertson, 1969; Wallace et al., 1988). Some other prominent studies along the same line include those models by Kashani and Saridis (1983), Lo et al. (2001), Yun and Park (2006), Stevanovic et al. (2007) and Liu and Chang (2011). Such a notion of delay minimization has also been adopted in later studies to tackle time-varying traffic dynamics with adaptive controls and real-time data (Christofa et al., 2016; Keyvan-Ekbatani et al., 2012; Aboudolas and Geroliminis, 2013; Keyvan-Ekbatani et al., 2013). Although some delay minimization models with mathematically elegant formulations have the potential to yield global optimal state (e.g., Lo et al., 2001), certain models, due to the nature of formulations, require the use of heuristic algorithms (e.g., genetic algorithms) to yield the near-optimal solution (e.g., Stevanovic et al., 2007; Liu and Chang, 2011). Also note that real-time control algorithms, compared to offline or time-of-day control systems, generally can better respond to traffic volume fluctuation and best use the available roadway capacity to minimize the congestion. However, most of such control systems remain at the demonstration stage and have not been adopted by most highway agencies up to date in the day-to-day operations even after the emerge of ITS for several decades. This is due not to their theoretical deficiencies, but mainly to their need for extensive real-time sensor information at the required level of accuracy and precision. The resources and personnel power essential to meet such needs and support their daily operations, however, are not affordable or sustainable at nearly all traffic agencies in U.S. Hence, a reliable and efficient time-of-day traffic control remains to be the most popular practice in the traffic community.

Featuring the properties to achieve the global optimality and display the results on the time–space diagram, those studies in the latter category attempt to provide a progression band for vehicles to traverse a set of consecutive intersections designed with optimally coordinated offsets. This core concept of progression, first developed by Morgan and Little (1964), is to maximize the green bandwidth so that most vehicles can encounter green phases over each arterial segment. Formulated with mixed-integer linear programming (MILP), Little (1966) further improved the model to concurrently optimize the cycle length, progression speed, and signal offsets. The enhanced version of their model, called MAXBAND, by Little et al. (1981), has accounted for the impacts of initial intersection queues and the sequence of left-turn phases on the effectiveness of the produced progression bands. Grounded on the core logic of MAXBAND, Gartner et al. (1991) proposed the Multiband model, which allows the bandwidths to vary with traffic volumes on different links. Chaudhary et al. (2002) further developed a progression optimization program, named PASSER, using different formulations but the same focus for bandwidth maximization. More later studies along the same line aimed to produce the optimized offsets, based on the

volumes over different links and the design of variable phase sequences (Messer et al., 1973; Wallace and Courage,1982; Chang et al., 1988; Papola, 1992; Tian and Urbanik, 2007; Li, 2013; Zhang et al., 2015; Arsava et al., 2016; Arsava et al., 2018). Note that the notion for traffic progression has also been refined and applied in the design of signal plans for unconventional intersections or traffic networks (Gartner and Stamatiadis, 2002; Gartner, 2004; Yang et al., 2014; Yang et al., 2016; Cheng et al., 2018; Yan et al., 2019).

However, despite the significant progress made by those studies, their focuses are mainly to improve the efficiency of the through movements along the arterial, thus often cannot achieve the desired level of performance for arterials connecting major intersections and accommodating heavy turning flows. All such turning flows, including outflows from and inflows to the arterial, may yield long queues and consequently impede the through movements due to the lack of designated progression bands. Hence, Yang et al. (2015) proposed a multi-path progression model to concurrently provide signal progression for the arterial's through movements and its turning paths based on the optimized signal offsets and phase sequences. Chen et al. (2019) have addressed a similar issue, but focused on analyzing the evolution of left-turn queues and their impact on the through progression bands with a model to free those progression bands from the impedance by the left-turn bay spillback. Notwithstanding the progress reported in the literature for improving the efficiency of arterial progression, most studies either require the OD information or have not yet accounted for the mutual blockage between through and turning flows moving in and out from the arterial. To contend with such critical issues, this study presents a MILP model to concurrently offer progression bands to all moving-in-and-out vehicles on each arterial link using only the information of each intersection's turning counts.

More specifically, the proposed model with the control objective of maximizing the total weighted bandwidths for all identified path flows offers a viable alternative for the design of signal progression for arterials accommodating such multi-path flow patterns with traffic data available from state-of-the-practice traffic sensors. Recognizing the availability of a great number of well-established models (Webster, 1958; Ackleik, 1981; MDOT SHA, n.d.) for optimizing cycle length and green splits at intersections, this study will focus on the optimization of offsets and phase sequences to generate progression bands for multi-paths of an arterial's traffic without the O-D information, and with the embedded constraints to prevent potential mutual blockages between different path flows. The produced progression bands under the optimized offsets and phases sequence can ensure that:

- Every major path flow over the arterial, defined as the volume level for a given path that is sufficiently high to fully utilize the specified minimal progression bandwidth or the minimum green duration, will be offered a progression band regardless of its travel distance;
- Each link, by accommodating the turning flows with the local progression band, can minimize the likelihood of experiencing turning bay overflows and the resulting mutual impedance between through and turn flows;
- The available green duration at each intersection is optimally allocated to the set of progression bands for optimally selected path flows based on their volumes;
- The through traffic flows over multiple links can take advantage of optimally connected local bands without suffering from the constraint of a negative correlation between the available progression bandwidth and its progression distance; and
- The entire arterial with the proposed control model can achieve the state of maximizing the total weighted progression band but not at the cost of any major path flow.

2. Modeling formulations

The proposed model, as shown in Fig. 4, employs MILP to formulate the following three sets of formulations for all local path flows between each pair of adjacent intersections so as to ensure their progression over the arterial:

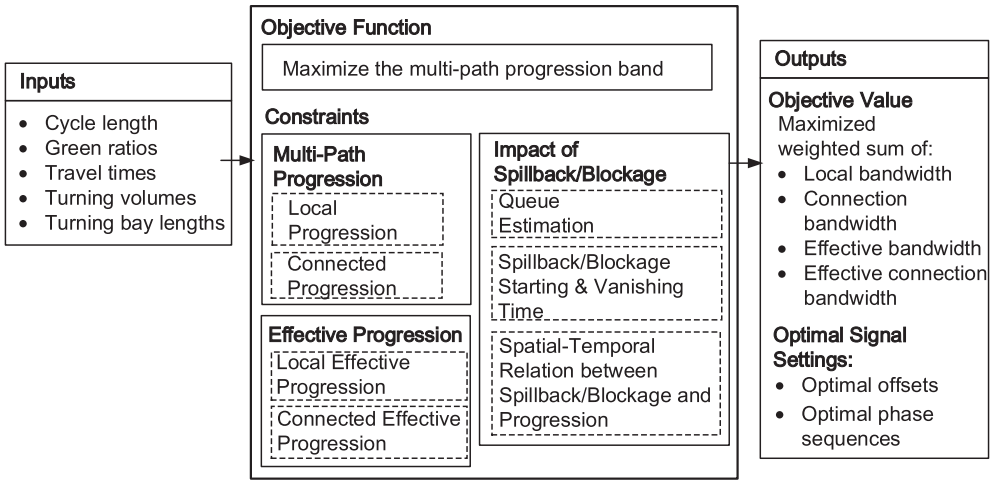

Fig. 4. Framework for the proposed multi-path progression model.

- **Constraints for Local Paths and Connections between Progression Bands**: to compute the local progression bands for all movements on each link and maximize the connection bands between two neighboring links, based on the optimized offsets and phase sequences.
- **Constraints of Effective Progression**: to estimate the portion of each local progression band and the connection band, respectively, that are not blocked by the queue spillback from other traffic movements.
- **Spatial and Temporal Evolution of the Turning and Through Queues**: to formulate the impacts of the turning and through queues formation/dissipation on the progression bands for all local paths so as to estimate the effective bandwidth for each local path.

A detailed discussion of all the above formulations for the outbound flows will be presented in the ensuing sections. One can follow the same logic and notations to derive the same set of formulations for the inbound flows.

2.1. Local progression bands for both through and turning movements

As shown in Fig. 5, a link with its upstream and downstream intersections constitutes the core building block:

$$\ell = (i,j)$$

The combination of upstream arriving and downstream departing traffic streams can generate up to nine local paths for one link. These local paths P are defined from p_1 to p_9 as shown in Fig. 5. More specifically, the traffic stream, entering and exiting the link via the movements of m and n is defined below as to take a local path$p$ for link ℓ:

$$p = (\ell, m, n) = (\ell, P) \tag{1}$$

Note that among the set of nine possible local paths p on a single link, the actual number of local paths within a link may vary with an intersection's geometric features and signal phasing plan. For example, if no left-turn movement at the downstream intersection is allowed, then $n \in \{\text{TH,RT}\}$, and p_2, p_5, and p_8 shall be removed from the list of available local paths. Also note that although each local path in Fig. 5 involves two intersections, such information in this study can be derived with only turning volume counts at each intersection, based on the assumption that all entry flows to a link will follow the field-measured average turning ratio to distribute the volumes at the downstream intersection. The key notations are listed in Table 1.

Fig. 6(a) shows an example of three local progression bands along local paths p_1, p_2, and p_4, between two neighboring intersections. Fig. 6(b) further illustrates the interrelationships between local progression bands and the signal phasing plans as well as durations at both the upstream and downstream intersections. Taking p_2 for example, its progression depends on the relations between the upstream through and the downstream left-turn green phases.

To ensure the progression for each local path on a link between two adjacent intersections, as shown in Fig. 6(b), one can formulate the following constraints for local paths with the same notion as for MAXBAND (Little et al., 1981):

$$v_p + b_p \le \widehat{\phi}_{\ell,m} \ \forall p = (\ell, m, n) \tag{2}$$

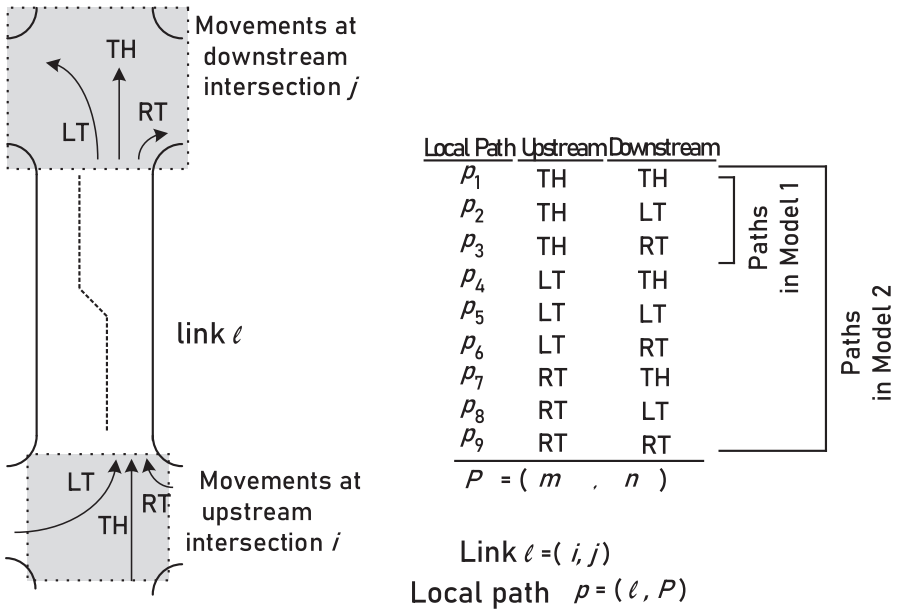

Fig. 5. Definition of local paths by upstream arrivals and downstream departures over a link.

Table 1
List of key notations.

Indices, Sets, and Operators	
m	Turning movement.$m \in \{\mathrm{LT}, \mathrm{TH}, \mathrm{RT}\}$
n	Turning movement. $n \in \{\mathrm{LT}, \mathrm{TH}, \mathrm{RT}\}$. Dummy variable $\bar{n}$ will be used when other movements coexist in the same equation.
$P = (m,n)$	Local paths, arriving as movement m and departing as movement n, on a link between two intersections.$P \in \{p_1, p_2, \cdots p_9\}$
$p = (\ell, m, n)$	Local path p defined as movement m arriving link ℓ and departs as movement n.
$\ell = (i,j)$	Link ℓ defined as a segment of arterial serving traffic from intersection i to intersection$j$
$\mathscr{A}(n)$	The set of downstream movements that can have some impact on movement n
$\mathscr{O}(\ell)$	The link that is in the oppose direction of link ℓ approaching the same intersection
$D(\ell)$	The link that is downstream of linkℓ
Parameters	
c	Common cycle length (sec)
$\widehat{\phi}_{\ell,m}(\phi_{\ell,n})$	The phase duration for movement$m(n)$ arriving(departing) link ℓ (sec)
b_0	Minimum bandwidth of value b_0 (e.g., 5 s in this study) (sec)
$s_{\ell,n}$	The saturation flowrate of movement n (veh/sec)
$\widehat{S}_p$	The dispersed flowrate for local path p (veh/sec)
$F_{\ell,m,\bar{n}}$	The flow rate of $\bar{n}$-movement's vehicles coming from the upstream movement m during green phase (veh/sec)
$q_{\ell,\bar{n}}$	The per-cycle outflow rate of movement $\bar{n}$ from link ℓ (veh/cycle)
$L_{\ell,\mathrm{LT}}$	The left-turn bay length on link ℓ (ft)
ρ^J	Jam density (veh/ft)
$N_{\ell,n}$	Number of lanes on link ℓ serving movement n (-)
T_p	Cruise travel time to complete the local path p (sec)
$T^B_{\ell,\bar{n}\to n}$	Travel time of through vehicles to traverse through the entire bay length of movement $\bar{n}$ or n on link ℓ (sec)
I	Inter-green duration (sec)
M	A large number for model computation needs in MILP
Variables	
Θ_j	Offset at the downstream intersection j of link ℓ (sec)
$\chi_\ell\left(\bar{\chi}_\ell\right)$	Binary variable indicating the phase sequence, which equals 1 if the green phase of the outbound through (left-turn) is before that of the inbound left-turn (through) (-)
$\theta_{\ell,n}(\widehat{\theta}_{\ell,m})$	The starting time of the green phase for the departure (inflow) movement n from (into) link ℓ (sec)
y_p	Binary variable which has value one if path p receives the progression and zero otherwise (-)
α_p	Binary variable, indicating the existence of an effective local band (-)
b_p	Bandwidth of path p (sec)
$v_p(w_p)$	The starting time of the effective local band at the upstream (downstream) intersection of link ℓ, calculated from the start time of a green phase (sec)
γ_p	The connection bandwidth from path p to the downstream path $D(p)$, via the through movement at the common intersection of those links (sec)
B_p	Effective local bandwidth for a local path p (sec)
$V_p(W_p)$	The starting time of the effective local band at the upstream (downstream) intersection of link ℓ, calculated from the start time of a green phase (sec)
$\tau_{\ell,n}$	Initial queue discharging time for outgoing movement n from link ℓ (sec)
Γ_p	Effective bandwidth for the connection bands (sec)
ω_p	The arrival time at the downstream intersection of the first vehicle following the path p (sec)
$Q_{\bar{n}\to p}$	The queue length of movement $\bar{n}$ when the path p first vehicle arrives at the downstream intersection (veh).$p = (\ell, m, n), n \neq n$
$t^O_{\bar{n}\to p}$	The time when the queues from movement$\bar{n}$ exceed the bay length and start to show some impacts on the progression band for a local path p (sec).$p = (\ell, m, n), n \neq n$
$t^R_{\bar{n}\to p}$	The time for the queues from movement $\bar{n}$ to end its impacts on vehicles traveling along path p (sec).$p = (\ell, m, n), n \neq n$
$\pi_{\ell,P}$	The path (ℓ, P) volume per cycle that can experience local progression (sec)
$\pi_{\ell,n}$	The volume per cycle that can experience local progression for movement n on linkℓ (sec)
$Y_{\ell,n}$	Maximum queue of movement n on link ℓ (veh)
K_p	Integer variable of path p such that the green phases of its upstream and downstream intersections are matched to the same cycle (-)

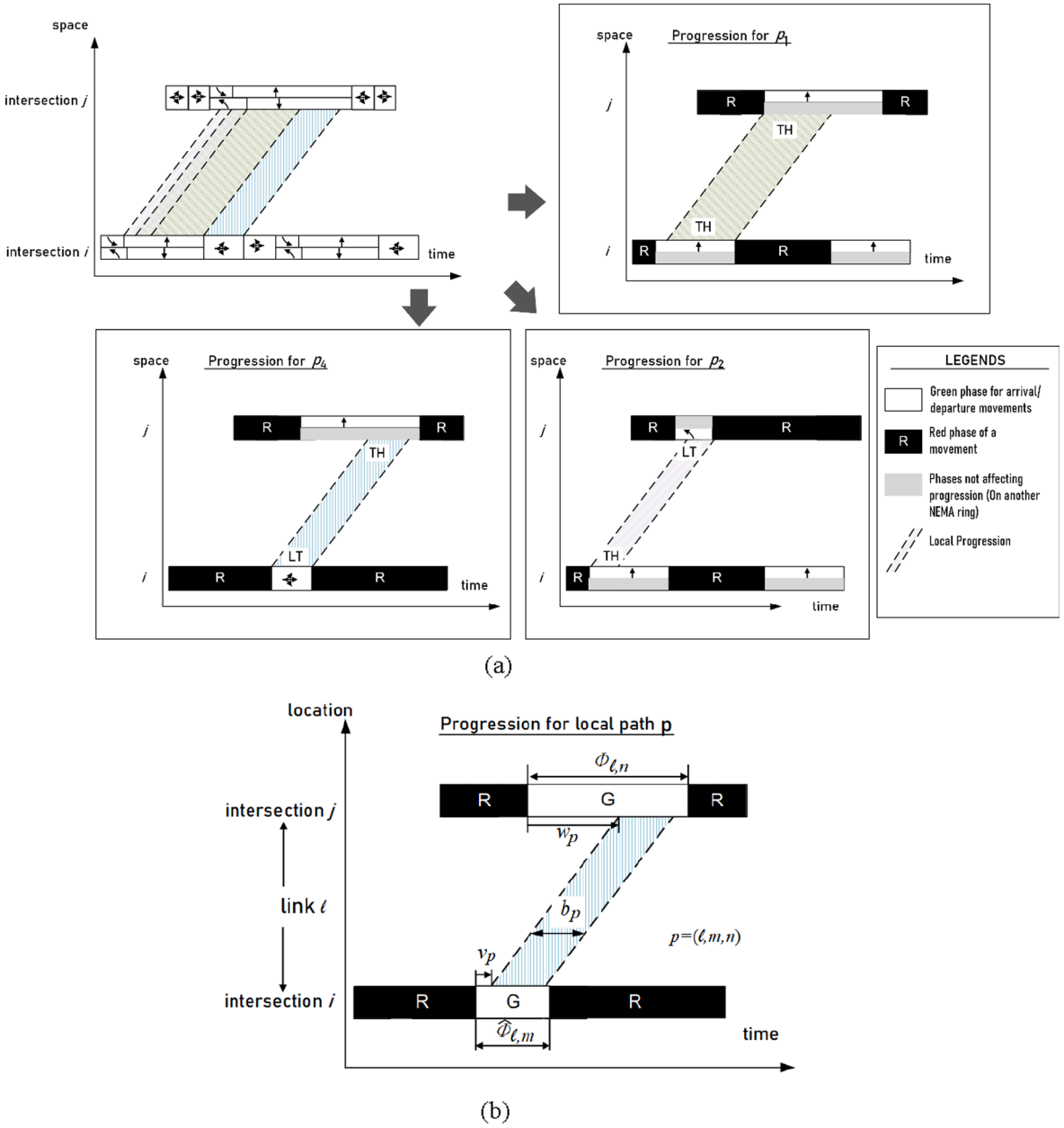

Fig. 6. Progression and connection of local paths (a) Three sample local bands between two intersections; (b) Progression for local path p; (c) Connection between local progression bands between two adjacent links; (d) Four possible patterns of the connected progression bands.

$$w_p + b_p \le \phi_{\ell,n} \ \forall p = (\ell, m, n) \tag{3}$$

$$w_p \ge \tau_{\ell,n} \ \forall p = (\ell, m, n) \tag{4}$$

where $\widehat{\phi}_{\ell,m}(\phi_{\ell,n})$ is the phase duration for movement$m(n)$ arriving(departing) link ℓ, $v_p(w_p)$ refers to the time difference between the start of a progression band for each local path and the corresponding green phase at the upstream (downstream) intersection of link ℓ; b_p is the local progression bandwidth; and $\tau_{\ell,n}$, is a variable, indicating the initial queue discharging time for outgoing movement n from link ℓ. Eqs. (2)–(4) serve as the interference constraints for the local progression.

To ensure that signals are synchronized between two intersections so that the vehicles would not be stopped within their designated local bands due to a red phase, one shall specify the following progression constraints for each local path$p$:

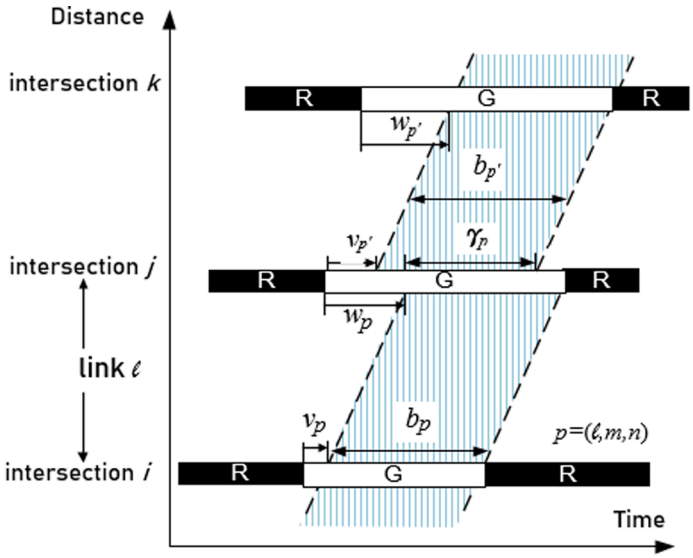

(c)

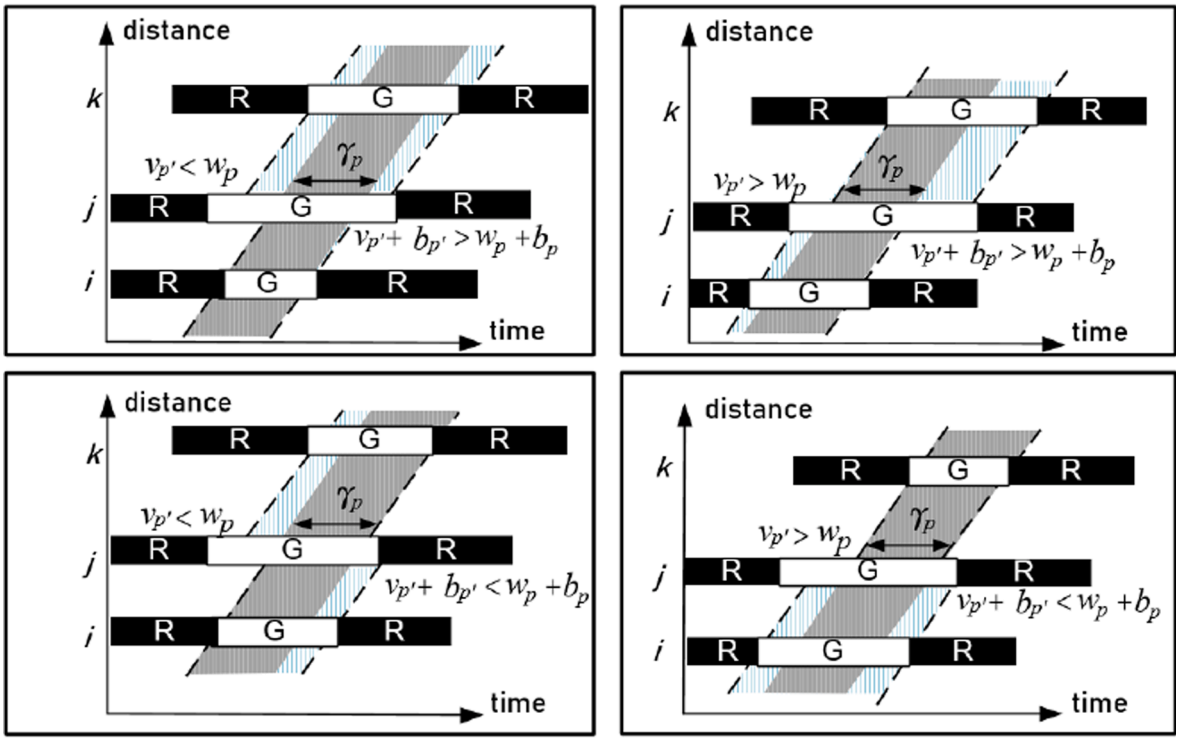

(d)

Fig. 6. (*continued*).

$$\widehat{\theta}_{\ell,m} + v_p + T_p = \theta_{\ell,n} + w_p + K_p \times c \;\forall p = (\ell, m, n) \tag{5}$$

where $\widehat{\theta}_{\ell,m}$ ($\theta_{\ell,n}$) is the starting time of the green phase for the inflow (departure) movement m (n) into link ℓ, respectively; T_p represents the travel time to complete the local path; K_p is an integer variable, and c refers to the signal cycle length.

For maximizing the total benefits of the entire arterial flows, it is conceivably not necessary for some path flows to receive local progression bands. Hence, only those path flows selected for progression should follow Eq.(5), and the binary variable,y_p, specified

below is used for the model to execute such a selection:

$$\widehat{\theta}_{\ell,m} + v_p + T_p \geq \theta_{\ell,n} + w_p + K_p \times c - M(1 - y_p) \quad \forall p = (\ell, m, n) \tag{6}$$

$$\widehat{\theta}_{\ell,m} + v_p + T_p \leq \theta_{\ell,n} + w_p + K_p \times c + M(1 - y_p) \quad \forall p = (\ell, m, n) \tag{7}$$

where M is a large number for model computation needs. When $y_p = 0$, Eqs. (6)–(7) are relaxed, indicating that the local band does not exist for local path p. Otherwise, the existence of the local band can be ensured with $y_p = 1$, for enforcing the integer loop constraints. The local paths selected for having progression bands can be identified as follows:

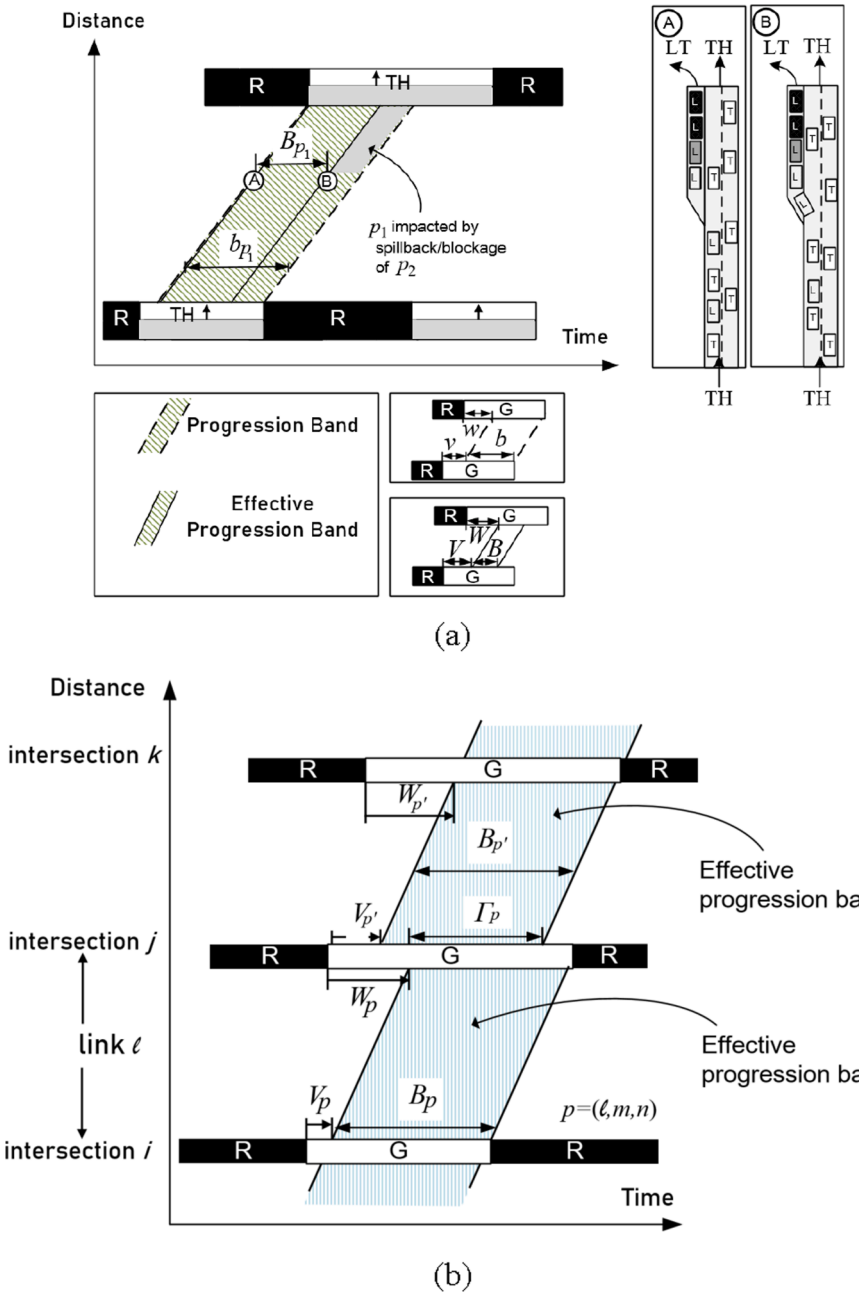

Fig. 7. Effective bandwidth not impacted by spillback/blockage; (b) effective band connection (c) Queue formation of left-turn and its impact on the through local path (p_1); (d) Queue formation of movement $\overline{n}$ and its impact on the local paths p; (e) relations between the onset of queue formation, fully discharging times, effective band, and conventionally-defined progression band;

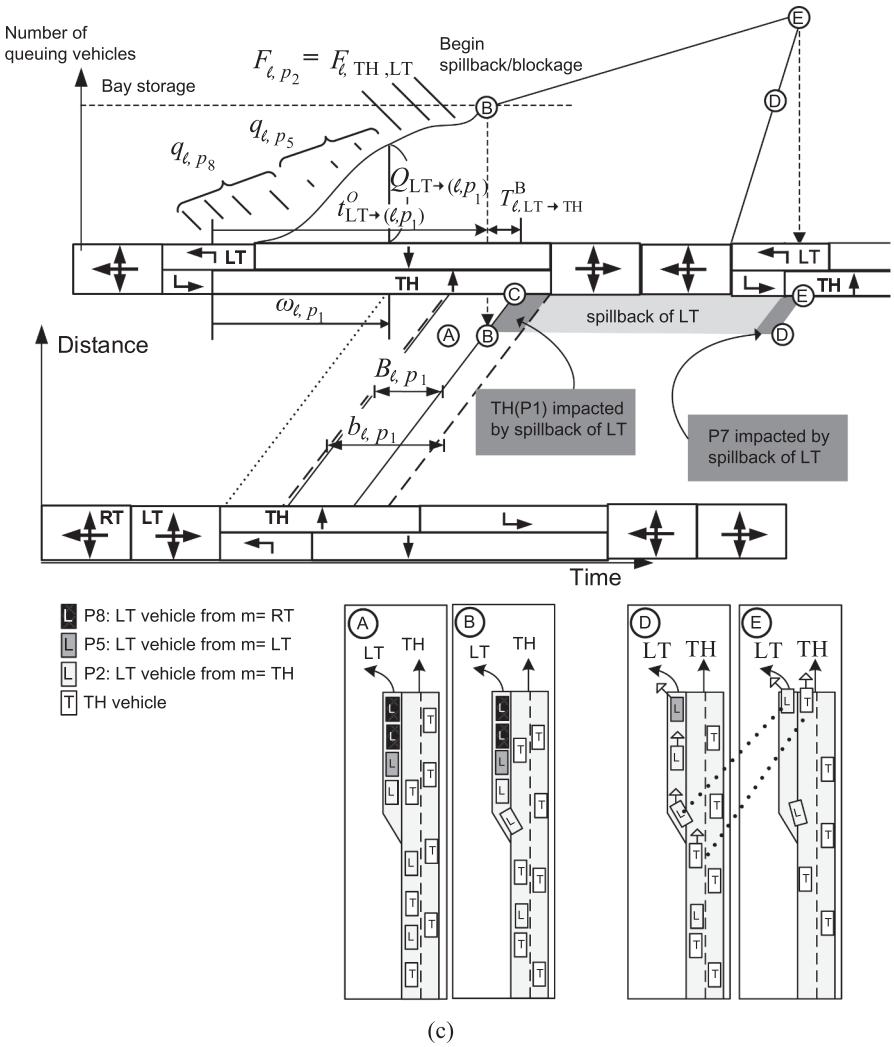

(c)

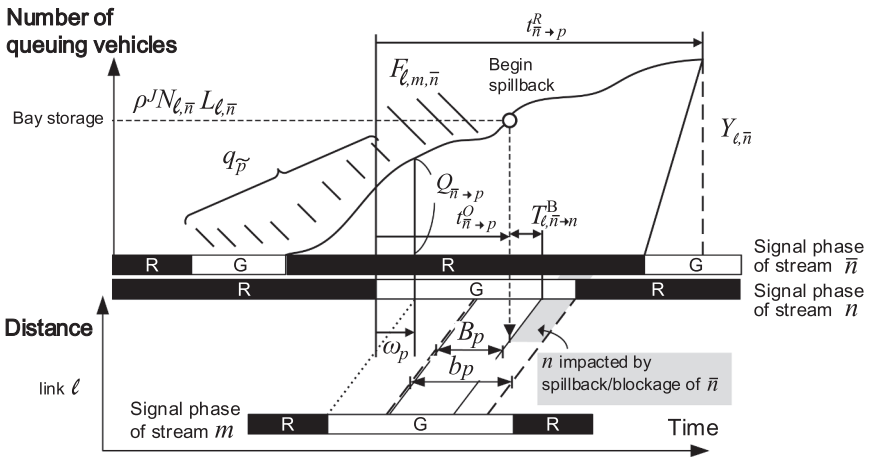

(d)

Fig. 7. (*continued*).

$$b_p \le M y_p \ \forall p \tag{8}$$

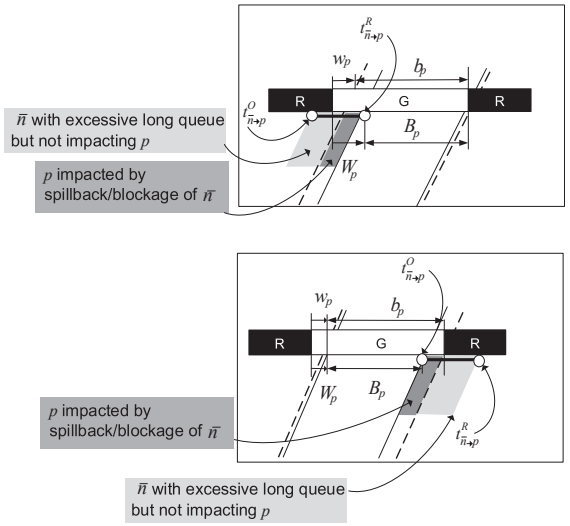

Fig. 7. (*continued*).

$$b_p \geq b_0 - M(1 - y_p) \ \forall p \tag{9}$$

where Eqs. (8) and (9) is to ensure the bandwidth for local path p either equals 0 when the band does not exist ($y_p = 0$) or is no less than a preset minimum bandwidth of value b_0 (e.g., 5 s in this study) when path p receives a local band ($y_p = 1$).

2.2. Connection between progression bands

Notably, the definition of local progression in this study is similar to the "partial progression opportunities" defined in Wallace and Courage (1982) for traveling between two intersections, but they can be connected for progression over a longer distance if designed properly. Since an intersection's departing flows via a local through band will naturally be the arrivals to its downstream link, as shown in Fig. 6(c), the design of local progression bands needs to include the optimal connection between two consecutive local bands for through movements.

To calculate the connection bandwidth, defined as the overlapped duration of the two local bands, one should adopt the following equation:

$$\gamma_p = \min\{w_p + b_p, v_{p'} + b_{p'}\} - \max\{w_p, v_{p'}\} \ \forall p = (\swarrow, m, n = \mathrm{TH}), \ p' \in D(p) \tag{10}$$

where γ_p denotes the connection bandwidth from path p to the downstream path $D(p)$, via the through movement at the common intersection of those links. Note that in Eq. (10), n can only be a through movement, but m and departing movements of p' can still be through or any turning movement. The overlapped duration, shown in Fig. 6(c), can be calculated with its starting and terminating times. The former can be selected from the upstream or downstream bands that have a later starting time. The same selection logic can be extended for the latter by referencing to the earlier ending time between the two progression bands. Fig. 6(d) shows the possible combinations of connected bandwidths, indicating that a vehicle can travel through at least three intersections (linking two pairs of intersections) over the connected progression bandwidth in the shaded regions in each of the four illustration panels.

2.3. The effective local bands not interrupted by the queue spillbacks

For a through movement along the arterial (p_1), its local band is likely to be impeded by the left-turn movement from the arterial to the crossing street (p_2). As shown in Fig. 7(a), the effective local band,B_p, shown with solid lines, is a portion of local band b_p, shown with dashed lines, but not blocked by the excessive queues. Such mutual relations can be expressed with the following constraints:

$$V_p \geq v_p \ \forall p \tag{11}$$

$$W_p \geq w_p \ \forall p \tag{12}$$

$$V_p + B_p \leq v_p + b_p \ \forall p \tag{13}$$

$$W_p + B_p \leq w_p + b_p \ \forall p \tag{14}$$

where B_p refers to the effective local bandwidth for a local path p and $V_p(W_p)$ is the starting time of the effective local band at the upstream (downstream) intersection of link ℓ (calculated from the start time of a green phase). Eqs. (11)–(14) ensure that the effective local band is less than its own local progression band. For example, Eq. (11) indicates that the effective band should start after the onset of local progression band, while Eq. (13) ensures the effective band to end before the end of the local band.

2.4. Effective band connection for through progression

Following the same notion of Eq. (10), Eq. (15) shows the effective bandwidth for the connection bands, the overlapped portion that allows vehicles to progress over consecutive links is shown with Eq. (15).

$$\Gamma_p = \min\{W_p + B_p, V_{p'} + B_{p'}\} - \max\{W_p, V_{p'}\} \ \forall p = (\ell, m, n = \mathrm{TH}), \forall p' \in D(p) \tag{15}$$

where Γ_p denotes the effective bandwidth for the connection bands, defined as the overlapped duration of two neighboring effective local bands, as illustrated in Fig. 7(b).

2.5. Formulations for estimating the impacts by the turning bay spillback

It should be noted the starting time and duration of the effective bands introduced in Eqs. (11)–(14) vary with the formation and dissipation of vehicle queues. For example, the impact of a left-turn (LT) queue spillback on a local through band along the arterial (p_1) on the same link should be estimated with the following two time points:

- $t^O_{\mathrm{LT}\to(\ell,p_1)}$: the time when the queues from the left-turn movement exceed the bay length and start to show some impacts on the progression band for a local path p_1 traverse the arterial;
- $t^R_{\mathrm{LT}\to(\ell,p_1)}$: the time for the queues from a left-turn movement to end its impacts on vehicles traveling along path $p_1$on the arterial.

The formulations in the next section are derived from this example (see Fig. 7(c)). The impacts of left-turn or through queues to other local bands can be formulated with the same logic and similar constraints.

2.6. The onset time to incur turning bay spillback or blockage

Note that the queue spillback from a left-turn bay will impact the band for the local through path along the arterial, as shown in Fig. 7(c). Such impacts can be estimated with the following steps:

Step 1: calculate the time point when the through path's first vehicle arrives at the downstream intersection, denoted by ω_{p_1}. The trajectory of the first vehicle following the through path is shown by the dotted lines in Fig. 7(c), and its arrival time at the downstream intersection, ω_{ℓ,p_1}, should be calculated with the offsets between two intersections and the travel time on the link, as expressed below (see Fig. 7(c)),

$$\omega_{\ell,p_1} = \widehat{\theta}_{\ell,\mathrm{TH}} + T_{\ell,p_1} - \theta_{\ell,\mathrm{TH}} - K_{\ell,p_1} \times c \tag{16}$$

Step 2: calculate the existing left-turn queue length when the through path's first vehicle arrives at the downstream intersection. Such left-turn queues are formed by vehicles from other local paths but arriving not within their local progression bands. As shown in Fig. 7(c), vehicles from both directions of the crossing street but not moving within their local bands contribute to such queues. Hence, the existing left-turn queues that may impact the through local path along the arterial can be expressed as follows:

$$Q_{\mathrm{LT}\to(\ell,p_1)} = \left(q_{\ell,p_5} - \pi_{\ell,p_5}\right) + \left(q_{\ell,p_8} - \pi_{\ell,p_8}\right) \tag{17}$$

where $Q_{\mathrm{LT}\to p_1}$ denotes the existing left-turn queue length when the through path's first vehicle arrives at the downstream intersection; $q_{\ell,P}$ is the volume per cycle of local path P on link ℓ; and $\pi_{\ell,P}$ is path volume per cycle that can experience local progression.

A general format of Eq. (17) is to sum up all the upstream flows contributing to the left-turn queue before any vehicle taking the through path arrives at the downstream intersection, and then exclude those experiencing local progression.

$$Q_{\mathrm{LT}\to(\ell,p_1)} = \sum_{\widetilde{m}\in\widetilde{\mathscr{M}}} q_{\ell,\widetilde{m},\mathrm{LT}} - \sum_{\widetilde{m}\in\widetilde{\mathscr{M}}} \pi_{\ell,\widetilde{m},\mathrm{LT}} \tag{18}$$

where $\widetilde{m} \in \widetilde{\mathscr{M}}$ denotes those upstream movements contributing to the left-turn queue before the first vehicle in the through path arrives at the downstream intersection, i.e., $\widetilde{m} \in \{\mathrm{LT}, \mathrm{RT}\}$ in this case.

Step 3: Calculate the remaining available space with the left-turn bay storage space and the existing left-turn queue, as follows:

$$\rho^J N_{\ell,\mathrm{LT}} L_{\ell,\mathrm{LT}} - Q_{\mathrm{LT}\to(\ell,p_1)} \tag{19}$$

where ρ^J represents the jam density; $N_{\ell,\mathrm{LT}}$ is the number of left-turn lanes on link ℓ; $L_{\ell,\mathrm{LT}}$ is the left-turn bay length on link ℓ;

Step 4: calculate the time for the left-turn queues to reach the bay length. During the period for vehicles on the through path to move along the link, these using the same upstream through green phase but turning left at the downstream intersection, would join the left-turn queue, as shown in time period A in Fig. 7(c). The accumulation rate of left-turn queue equals the flow rate of those taking the path, comprising a through movement from the upstream intersection and a left-turn at the link's downstream intersection. Therefore, one can show the starting time for the left-turn queues to reach the end of the bay and to impede the flows on local through path as follows:

$$\frac{\rho^J N_{\ell,\mathrm{LT}} L_{\ell,\mathrm{LT}} - Q_{\mathrm{LT}\to(\ell,p_1)}}{F_{\ell,\mathrm{TH,LT}}} \tag{20}$$

where $F_{\ell,TH,LT}$ is the flow rate of left-turn vehicles coming from the upstream through green phase. Note that one can model the effect of right-turn-on-red (RTOR) by including the volumes of right-turners from upstream crossing street utilizing the green phase of the upstream intersection's through movement in $F_{\ell,TH,LT}$. Specifically, one should add the RTOR volumes of path p_7 to $F_{\ell,TH,LT}$. With such change, Eq.(20) would yield a lower value, implying that the left-turn queues will build up sooner when RTOR traffic, or even other mid-block traffic, is present. On the other hand, right-turn traffic on the arterial is not subjected to RTOR constraints since right-turners can receive progression along with the through movement by sharing the same green phases.

Step 5: calculate the time for the left-turn queues to show their impacts on the through local band. The time point when the queues for the left-turn movement exceed the bay length and start to partially block the progression band for the local through path p_1 can be formulated with the following constraint:

$$t^O_{\mathrm{LT}\to(\ell,p_1)} = \frac{\rho^J N_{\ell,\mathrm{LT}} L_{\ell,\mathrm{LT}} - Q_{\mathrm{LT}\to(\ell,p_1)}}{F_{\ell,TH,LT}} + \omega_{\ell,p_1} + T^B_{\ell,\mathrm{LT}\to\mathrm{TH}} \tag{21}$$

where $T^B_{\ell,\mathrm{LT}\to\mathrm{TH}}$is the time period between onset of the spillback and the starting time of the impact to the local band, which equals the travel time of through vehicles to traverse through the entire bay length. The last term in Eq. (21), $T^B_{\ell,\mathrm{LT}\to\mathrm{TH}}$, accounts the fact that after the left-turn queue spillback occurs, the progression can sustain until the last unimpeded vehicle arrives at the stop bar, as shown in the duration between time points B and C in Fig. 7(c).

Note that the critical timing of incurring spillback, $t^O_{\mathrm{LT}\to(\ell,p_1)}$, maybe negative, indicating the worst case that spillback already happened before the arrival of these vehicles within their progression bands. On the contrary, it may also be a number larger than the cycle length, indicating that the spillbacks are rather unlikely to occur.

Grounded in the same notion, one can also derive the above formulations for all other local paths likely impacted by the queues from other paths. To do so, this study adopts the compressed notations with n denoting the set of movements suffering from the queue blockage, and $\bar{n}$ denoting the set of movements generating queues (See Fig. 7(d)). Specifically, all potential conflicts between the queues and a local band include:

- when $n = \mathrm{TH}$, $\bar{n} \in \{\mathrm{LT}, \mathrm{RT}\}$, indicating that through stream may be impacted by left- or right-turn queue spillbacks;
- when $n \in \{\mathrm{LT}, \mathrm{RT}\}$, $\bar{n} \in \{\mathrm{TH}\}$: indicating that right- and left-turn stream may be impacted by through queue spillbacks.

With the above notations, one can formulate the time when spillback of the queue of $\bar{n}$ starts impacting the band of local path p with the following general expressions:

$$\omega_p = \widehat{\theta}_{i,m} + T_p - \theta_{\ell,n} - K_p \times c \;\; \forall p = (\ell, m, n) \tag{22}$$

$$Q_{\bar{n}\to p} = \sum\nolimits_{\widetilde{p}=(\ell,\widetilde{m},\bar{n})} q_{\widetilde{p}} - \pi_{\widetilde{p}} \;\; \forall p = (\ell, m, n),\;\; \bar{n} \in \mathscr{A}(n) \tag{23}$$

$$t^O_{\bar{n}\to p} = \frac{\rho^J N_{\ell,\bar{n}} L_{\ell,\bar{n}} - Q_{\bar{n}\to p}}{F_{\ell,m,\bar{n}}} + \omega_p + T^B_{\ell,\bar{n}\to n} \;\; \forall p = (\ell, m, n),\;\; \bar{n} \in \mathscr{A}(n) \tag{24}$$

where $\mathscr{A}(n)$ refers to the set of downstream movements that can have some impact on movement n.

2.7. Estimating the number of vehicles within the progression bands

One key issue in Eq. (23) is how to compute those vehicles in the progression band so as to better estimate the resulting queues. Note that vehicles can progress over all lanes if moving within their effective local band; otherwise, they can only use those lanes not blocked by excessive queues, if within the remaining portion of the band. Hence, the number of vehicles within and out of the effective local bands should be computed. The former is the product of bandwidth and the discharge rate, and the latter must be modified by a

term, reflecting the impact of excessive queues on one lane in a local path. Therefore, such vehicles can be calculated with Eq. (25) as follows:

$$\pi_p = B_p \widehat{S}_p + \left(b_p - B_p\right) \times \frac{N_{\ell,n} - 1}{N_{\ell,n}} \times \widehat{S}_p \ \forall p = (\ell, m, n) \tag{25}$$

where $\widehat{S}_p$is the dispersed flowrate for local path p. When estimating the potential discharge rate, one should notice that a vehicle platoon discharged at the saturation flow rate from an upstream stop line may not necessarily sustain such a high flow rate at the downstream intersection. Therefore, this study takes Robertson's platoon dispersion effect (Robertson, 1969) into consideration, by adopting the dispersed flowrate $\widehat{S}_p$ for the potential discharge rate at the downstream intersection.

2.8. The fully discharging time for vehicles in the queue spillbacks state

The local progression band can be recovered once the queues causing spillback are fully discharged. With the same definition for set $\overline{n}$ as in the last section, the time for a local band for movement n to be free from the impacts of entire queues of $\overline{n}$, as shown in Fig. 7(a), can be expressed as follows:

$$t^R_{\overline{n}\to p} = \theta_{\ell,\overline{n}} - \theta_{\ell,n} + \tau_{\ell,\overline{n}} \ \forall p = (\ell, m, n), \ \overline{n} \in \mathscr{A}(n) \tag{26}$$

where $\tau_{\ell,\overline{n}}$ is the discharging time of the initial queue defined in (4). Notably, the ending time of blockage is referred to the time instant when the last queueing vehicle has reached the stop bar (that is when the entire queue has been discharged), which can be calculated with Eq. (27). The time for such a vehicle (with movement $\overline{n}$) to reach the stop line is also the time when the first blocked vehicle (with movement n) in the progression band reaches the stop line after the blockage vanished on the travel lane. Specifically, although label D in Fig. 7(c) indicates when spillback diminishes at the upstream end of the turning bay, the time instant indicated by label E is viewed as the ending time of the bay blockage in Eq. (27).

$$\tau_{\ell,\overline{n}} = \frac{Y_{\ell,\overline{n}}}{s_{\ell,\overline{n}} \times N_{\ell,\overline{n}}} \ \forall \overline{p} = (\ell, m, \overline{n}) \tag{27}$$

where $s_{\ell,\overline{n}}$ is saturation flowrate of movement $\overline{n}$; and $Y_{\ell,\overline{n}}$ is a variable indicating the maximum queue (in number of vehicles) of movement $\overline{n}$, which can be estimated from those volumes not enjoying the progression band for movement$\overline{n}$:

$$Y_{\ell,\overline{n}} = q_{\ell,\overline{n}} - \pi_{\ell,\overline{n}} \ \forall \ell, \ n \in \mathscr{A}(n) \tag{28}$$

where $q_{\ell,\overline{n}}$ is the per-cycle outflow rate of movement $\overline{n}$ from link ℓ, and $\pi_{\ell,\overline{n}}$ is the per-cycle outflow rate receiving progression of movement $\overline{n}$ from link ℓ. Following the logic in (23), vehicles that can experience progression are also excluded from the calculation of the queue length, as shown with the last two terms. It should be noted that some vehicles not in the progression band designed with conventional models (Little et al., 1981; Gartner et al., 1991; Yang et al., 2015; and Arsava et al., 2016) may not be necessarily stopped on each red phase, but the vehicles not in their designated local paths' progression band will inevitably be stopped at the immediate downstream intersection.

2.9. Spatial and temporal relations between the queue spillbacks and local progression bands

Given the starting and ending time points for the queue spillback to impact the local bands, one can formulate their spatial–temporal relations with a set of constraints. The effective bands, excluding the duration when progression band is blocked by spillback queues, can be expressed with the following equations:

$$W_p + M\left(1 - \alpha_p\right) \geq t^R_{\overline{n}\to p} \ \forall p = (\ell, m, n), \ \overline{n} \in \mathscr{A}(\boldsymbol{n}) \tag{29}$$

where α_p is a binary variable, indicating the existence of an effective local band;

By the same token, the effective band that can sustain until the next overflow occurs can be expressed with Eq. (30)

$$W_p + B_p \leq t^O_{\overline{n}\to p} + M\left(1 - \alpha_p\right) \forall p = (\ell, m, n), \ \overline{n} \in \mathscr{A}(\boldsymbol{n}) \tag{30}$$

Eqs. (29)–(30) would be relaxed when $\alpha_p = 0$, indicating that the effective local band does not exist, and such conditions can be identified by the following relation:

$$M\alpha_p \geq B_p \ \forall p \tag{31}$$

On the other hand, the possible cases of nonzero effective bandwidth ($\alpha_p = 1, B_p > 0$), as a portion of conventionally-defined progression band, depending on the onset and fully discharge time of the queue blockage are summarized in Fig. 7(e) based on Eqs. (12), (14), (29)–(31). Note that in Fig. 7(e), the gray areas indicate the duration when the movement $\overline{n}$ has exhibited excessive long queue, but only within the dark gray areas would path p be impacted by the movement $\overline{n}$.

2.10. Temporal relations between a green phase's starting time and the Intersection's offset

Recognizing the availability of a great number of well-established models (Webster, 1958; Ackleik, 1981; MDOT SHA, undated) for optimizing cycle length and green splits at intersections, this study will focus on the optimization of offsets and phase sequences to achieve the proposed control objectives. Note that the starting time of the green phase for each movement should be computed concurrently with optimization of the intersection's offsets and the phase sequence. The constraints for doing so for each movement as used in MAXBAND (Little et al., 1981) and Multiband (Gartner et al., 1991) can be specified as follows:

$$\theta_{\ell,\mathrm{TH}} = \Theta_j + (1-\chi_\ell)\bullet\left(\phi_{\mathscr{O}(\ell),\mathrm{LT}} + \mathrm{I}\right)\ \forall \ell = (\mathrm{i},\mathrm{j}) \tag{32}$$

$$\theta_{\ell,\mathrm{LT}} = \Theta_j + \left(1-\overline{\chi}_\ell\right)\bullet\left(\phi_{\mathscr{O}(\ell),\mathrm{TH}} + \mathrm{I}\right)\ \forall \ell = (\mathrm{i},\mathrm{j}) \tag{33}$$

where Θ_j is the offset at the downstream intersection j of link ℓ; $\mathscr{O}(\ell)$ refers to the inbound link (with opposed direction to link ℓ)at the upstream of intersection j; $\chi_\ell\left(\overline{\chi}_\ell\right)$ is a binary variable indicating the phase sequence, which equals 1 if the green phase of the outbound through (left-turn) is before that of the inbound left-turn (through); and I is inter-green time. Fig. 8 shows how the possible phase sequences can be arranged from binary variables in Eqs. (32)–(33). The side street signal phases can also be formulated by the same token.

Notably, despite a large number of variables in Table 1, most variables can be computed with the signal offsets and phase sequences via those formulated equations.

2.11. Upper bound for effective bandwidth

Considering that the bandwidth wider than needed should be distributed to other movements if possible, one should set the following upper bound for each effective local band:

$$B_p\widehat{S}_p \le q_p\ \forall p = (\ell,m,n), \ell = (i,j) \tag{34}$$

Eq. (34) ensures that the effective local bandwidth would not be wider than the discharge time for all vehicles in local path p.

2.12. Path volumes

Volume on each local path used in the proposed methodology for producing the multi-path progression bands, as shown in Eqs. (35) and (36), can be derived directly from each intersection's turning counts without the O-D flow information:

$$q_p = q_{\ell,m}\bullet q_{\ell,n}\Big/\sum\nolimits_{\bar{n}} q_{\ell,\bar{n}}\ \forall \mathrm{p} = (\ell,\mathrm{m},\mathrm{n}) \tag{35}$$

$$q_{p,p'} = q_p\bullet q_{\ell',n}\Big/\sum\nolimits_{\bar{n}} q_{\ell',\bar{n}}\ \forall \mathrm{p} = (\ell,\mathrm{m},\mathrm{TH}),\ \mathrm{p}' = (\ell',\mathrm{TH},\mathrm{n}) \in \mathrm{D}(\mathrm{p}) \tag{36}$$

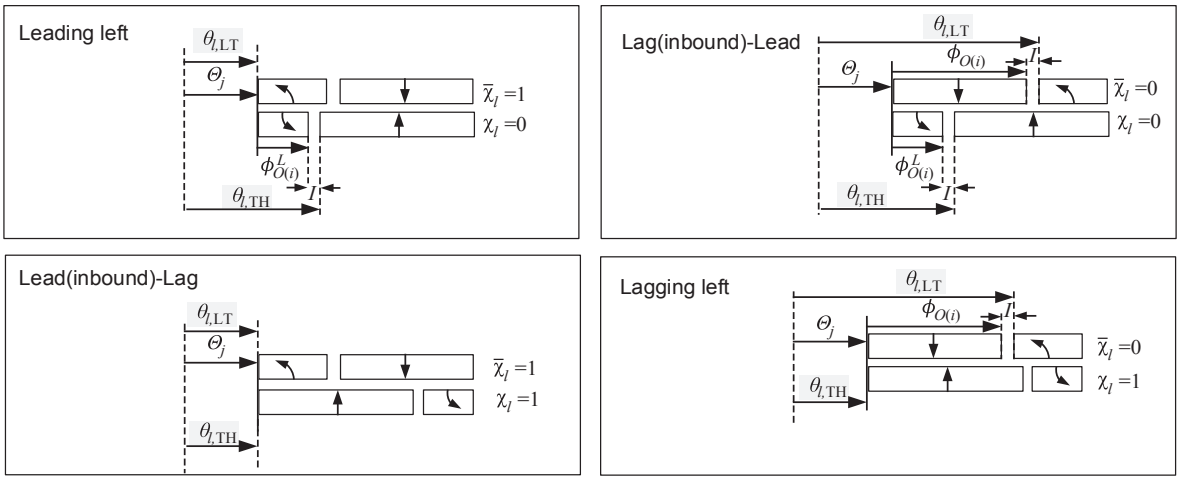

Fig. 8. Graphical illustration of possible signal phase sequences.

Note that Eqs. (35) and (36) are developed under the assumption that a link's entry flows regardless of from which traffic stream, will distribute at the link's downstream intersection based on the average turning ratios computed from field traffic counts.

Also note that only using intersection turning volume counts, the proposed model will distribute the green durations to possible major paths with the volumes identified with Eqs. (35) and (36), which, however, may not always be identical to the results based on those (unobservable) true paths.

Fig. 9(a) shows an example with known turning volume counts. Pattern 1 is with prevailing paths A and B, while Pattern 2 is with paths C and D (other path flows are omitted in the figure). It is conceivable that Patterns 1 and 2 are with completely different major paths, which is unknown to the proposed model but *assumed to be known* in Multipath (Yang et al., 2015) or OD-BAND (Arsava et al., 2016). The limitation of the proposed model is that given the only accessible input of intersection turning counts, but without the information of true path-flow pattern and their volume distributions, it will allocate available green durations to all possible paths

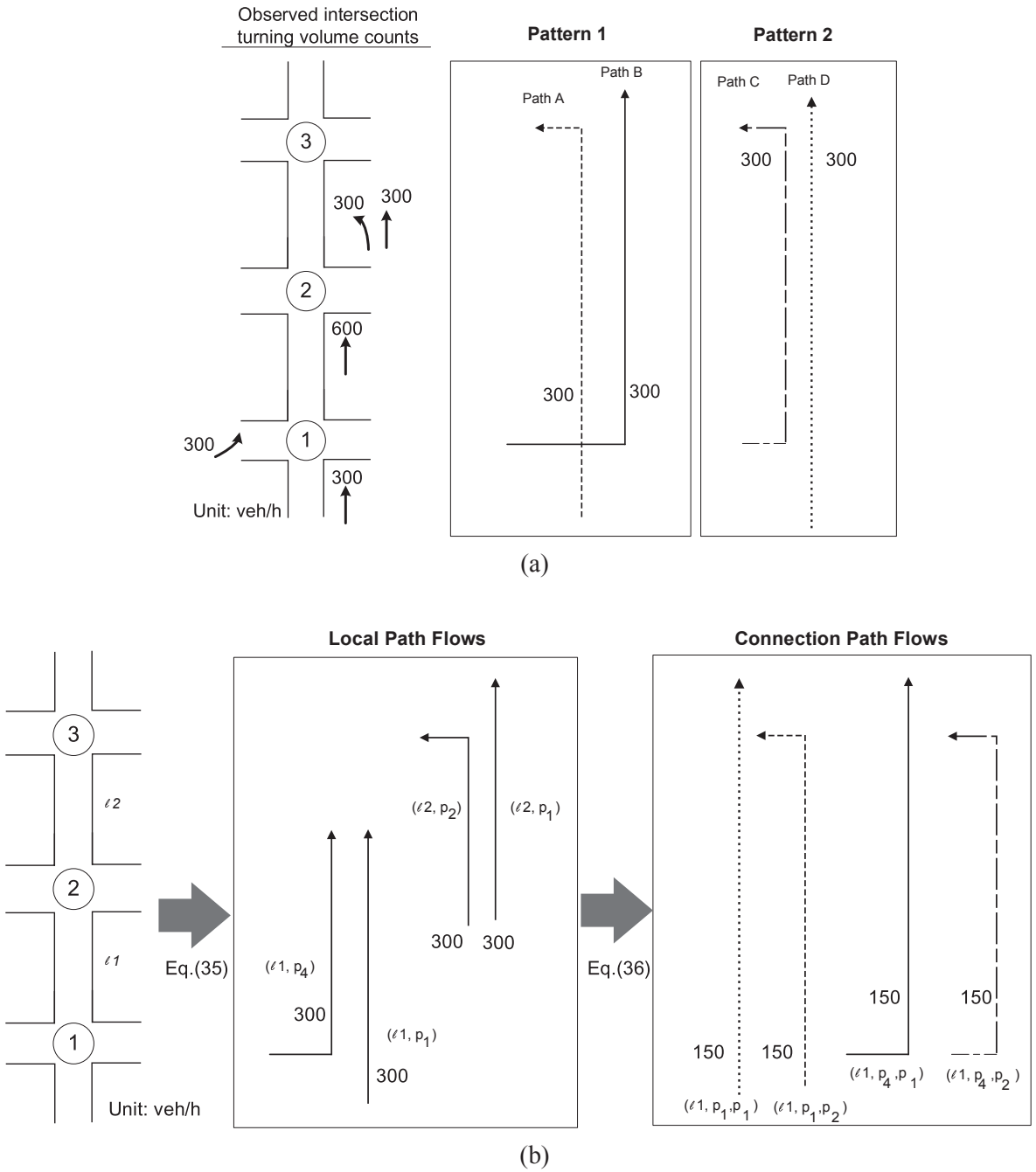

Fig. 9. Different path-volume patterns albeit given the same intersection turning volume counts; (b) patterns with the proposed method.

based on their volumes estimated from the turning counts. Certainly, such results may not be optimal, compared with the one with *perfect information*, but are implementable in practice for offline control, or can be as the basis for real-time system operations.

For example, the proposed model strives to provide satisfactory progression for all paths (A, B, C, and D) in the signal design. Eq. (35) first generates local path flows, and Eq. (36) further produces connection path flows, as shown in Fig. 9 (b). The connection path flows generated from only turning volume counts, although unable to identify pattern 1 or 2, or any patterns other than patterns 1 and 2, are adopted to optimize the signal to provide progression to all the possible paths, with volumes of 150(veh/h) each. Indeed, such results cannot guarantee the best performance for a given known path flow pattern, but it will be the most robust signal plan considering that the actual pattern is practically unknown.

2.13. Objective function

The objective of the proposed model is to maximize the sum of all bandwidths for the selected local paths weighted by their respective volumes. These weights are used to reflect the number of vehicles that can benefit from their designated bands. For example, the portion of the local band interrupted by turning bay spillback or blockage can only benefit these vehicles in the non-impeded lanes. Therefore, the objective function can be expressed as follows:

$$\mathrm{Max}\sum_{p} \mu_p^1 \bullet \mathrm{B_p} + \mu_p^2 \bullet \Gamma_\mathrm{p} + \mu_\mathrm{p}^3 \bullet \left(\mathrm{b_p} - \mathrm{B_p}\right) + \mu_\mathrm{p}^4 \bullet \left(\gamma_\mathrm{p} - \Gamma_\mathrm{p}\right)\ \forall \mathrm{p} \tag{37}$$

where μ_p^z are the weighting factors based on traffic volumes on local path p.

$$\mu_p^1 = q_p \times \widehat{S}_p\ \forall p \tag{38}$$

$$\mu_p^2 = q_{p,p'} \times \widehat{S}_p\ \forall p, p' \in D(p) \tag{39}$$

$$\mu_p^3 = q_p \times \frac{N_{\ell,n} - 1}{N_{\ell,n}} \widehat{S}_p\ \forall p = (\ell, m, n) \tag{40}$$

$$\mu_p^4 = q_{p,p'} \times \frac{N_{\ell,n} - 1}{N_{\ell,n}} \widehat{S}_p\ \forall p = (\ell, m, n) \tag{41}$$

Although all those nine paths are considered in Eq. (37), some of them may not be assigned with progression bands under the control objective of maximizing the system's total bandwidths. The final set of paths selected for progression vary with the optimized value of the binary variable α_p, which may include some or all of those nine possible paths. As such, the traffic queues on those paths not receiving progression bands have been accounted for in the proposed model's formulations and constraints to minimize their impacts on the arterial system's overall effectiveness.

Also note that the progression band is not limited to the direction of heavy flows since the proposed model is capable of finding the weighted bandwidths for both directions on the arterial. Under the framework of MAXBAND, the offsets and phase sequences are optimized at each intersection concurrently for both directions. With the objective function that adopts the weighted bidirectional bandwidths and essential constraints to capture the interrelations between intersections, all control variables for all intersections will be solved concurrently.

In summary, the proposed models with all above formulations can concurrently provide maximized progression for all selected paths along an arterial under the given geometric constraints and offer the best connection for all path flows between adjacent links

Table 2
Experiment settings.

	Experiments		
	1	2	3
Purpose	• Compare the results generated from the benchmark and proposed models (signal plans, bandwidths) • Compare the performance using microscopic simulation model as the evaluation platform	Show that the proposed model, circumventing the need to use the rarely available arterial O-D volume distributions, can yield a comparable level of performance.	Confirm that allowing the variable phase sequence and including turning volumes from side streets to the arterial's progression design can yield better control effectiveness.
Scenario (s)	Field data	Three scenarios with different path volumes (summarized in Table 8) but the same turning volume counts at each intersection from the field data	With various volume levels
Model(s)	• TRANSYT (Binning, 2019) • Multiband (Gartner et al., 1991) • Model 1 • Model 2	• Multiband (Gartner et al., 1991) • Multipath (Yang et al., 2015) • Model 2	Model 2

using only the readily available information of intersection turning counts, rather than the O-D volume distribution.

3. Case study

For performance evaluation, this study has conducted extensive simulation experiments and numerical analysis with respect to the following issues:

- The arterial under the control objective of maximizing progression for multiple local paths will not be at the expense of other measures of effectiveness (MOEs);
- The turning-in volumes from crossing streets to the arterial need to be included in the design of the signal progression plan to ensure its effectiveness; and
- Both the arterial's through and the turning flows under the proposed optimized phase sequence and offsets can concurrently have their designated progression bands over consecutive intersections.
- The proposed model, although adopting only turning volume counts, can yield the performance level comparable to the state-of-the-art path-based progression model operated with the given O-D volume distributions.

Some additional sets of numerical experiments, summarized in Table 2, have also been conducted for evaluating the proposed model's responsiveness on (1) providing wider progression bands to turning movements of higher volumes; (2) minimizing the queue spillback likelihood in design of signal plan; and (3) utilizing the variable phase sequence to best the model's overall performance.

The study site for the case study is an arterial segment of six intersections on MD187 (Old Georgetown Rd.) in North Bethesda, MD. Fig. 10(a) shows its geometric features, including link lengths, bay lengths, and the number of lanes, right-turn type (unsignalized, no-turn-on-red, or l right-turn-on-red). Derivations of model inputs are listed in Table 3, using intersection turning counts, critical lane

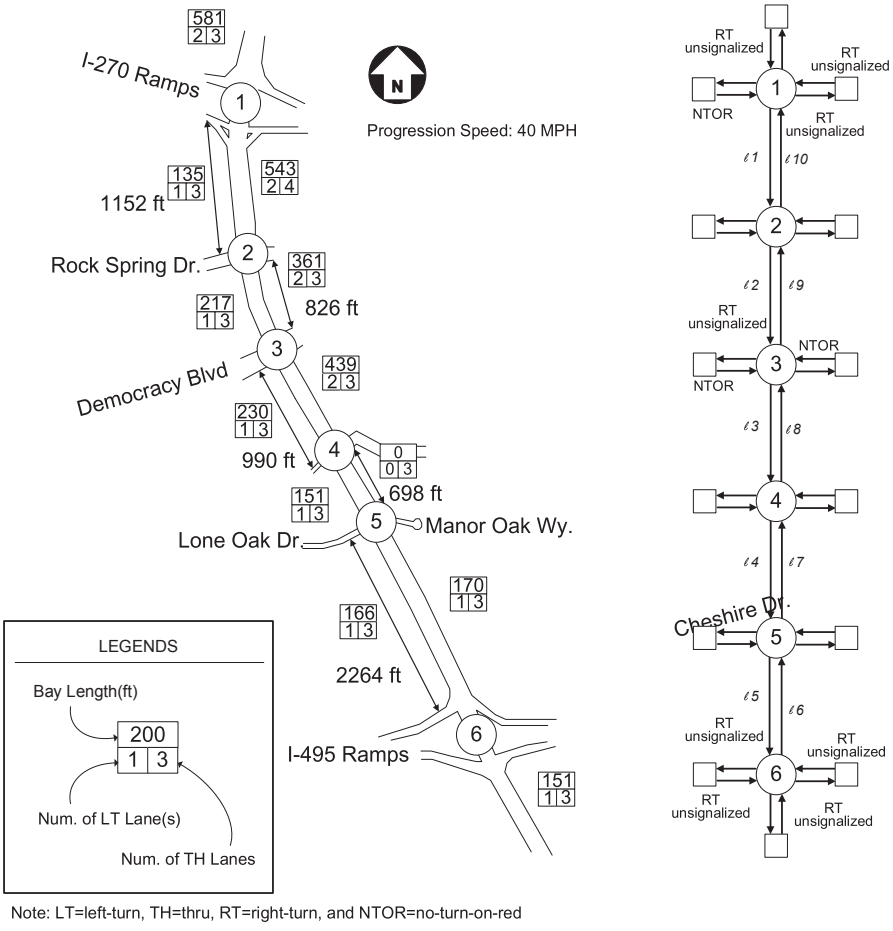

(a)

Fig. 10. Key field data associated with the study site: (a) geometric features; (b) hourly-turning volumes and; (c) signal timings (Num. = Number, LT = Left-turn, and TH = Through).

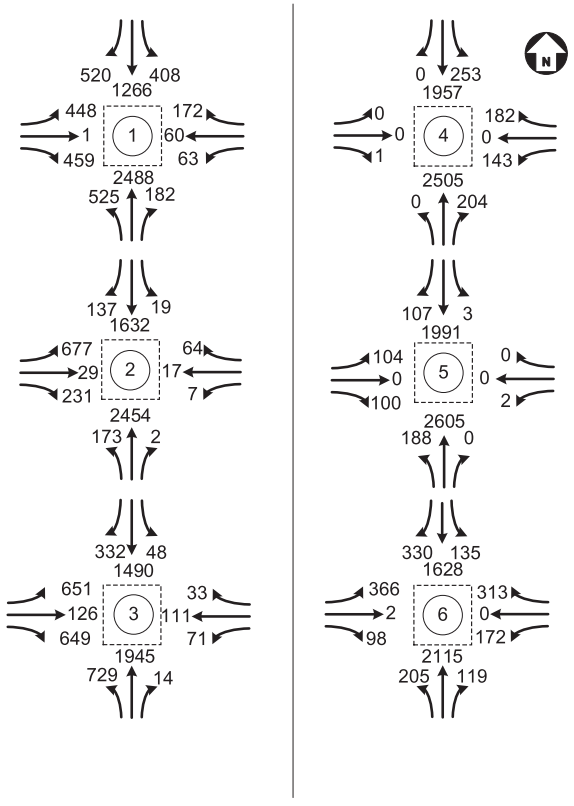

(b)

Fig. 10. (*continued*).

volume methods (or alternatively one can apply HCM methodology (HCM, 2016)), and satellite images, as used by most state agencies.

All intersection approaches on the arterial, except northbound of intersection 4, have left-turn bays, whose lengths and the number of lanes are shown in Fig. 10(a). For example, the northbound approach of intersection 2 has a left-turn bay with two lanes and is 361 (ft) in length.

Fig. 10(b) illustrates the hourly turning volume counts during the evening peak period. Fig. 10(c) presents the green splits and cycle length computed in advance with the critical lane volume method commonly used by the traffic community (e.g., MDOT SHA), while signal offsets and phase sequences are variables to be optimized by the benchmark and proposed models.

As shown in Fig. 10(c), the number of signal phases ranges from four to six, where intersections 1, 2, 3, and 6 have six phases and operate with either leading, lagging, or lead-lag for left-turn phases on the arterial and with split phasing for crossing streets. Intersections 4 and 5 are without protected left-turn phase for those directions with low left-turn demand. At these two intersections, eastbound and westbound movements share the same phase. Also note that right-turn overlapping phases are applied at intersections 1, 2, 3, and 5, i.e., eastbound right-tuners receive protected right-turn arrows during the northbound protected left-turn. Therefore, these right-turning vehicles may receive progression within two phases.

Recognizing that a simulated system is convincing only if it can reflect actual traffic patterns, this study has performed the calibration on traffic volumes. Path flows obtained from the simulation are examined to conform with the field-collected data for the need of simulation, and Table 4 shows the calibration results for selected paths, including the Geoffrey E. Havers (GEH) test values for the baseline scenario in experiment 1 and all scenarios with different levels of path-flow volumes in experiment 2.

3.1. Experiment 1: Simulation evaluation

Using VISSIM 9 (PTV, 2016), a well-calibrated microscopic simulation model, as the evaluation platform, this study has selected the following models for performance comparison.

- TRANSYT 16: a state-of-the-art network signal optimization software tool (Binning, 2019)
- Multiband: a state-of-the-art progression model (Gartner et al., 1991) to serve as the benchmark.
- Model 1: the proposed model, but excluding the constraints related to turning-in flows from the crossing streets. Specifically, the inflow to links in Eqs. (1)–(15), (22)–(26), (29)–(31), (34) are confined to only through flows.
- Model 2: the proposed model with all essential constraints in the formulations.

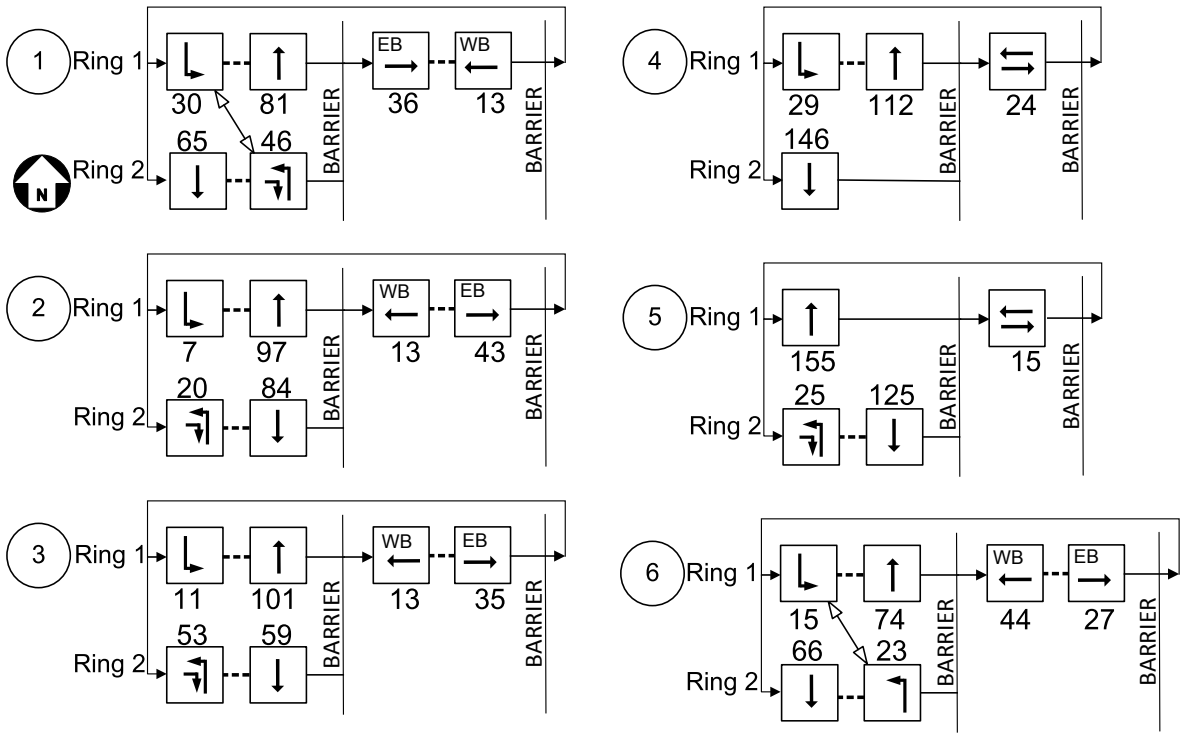

Notes:
a) EB=eastbound; WB=westbound
b) Green duration in seconds
c) Intergreen: 5 seconds between all phases
d) Two phases sharing the same dashed line are allowed to switch their sequence during phase sequence optimization.
e) Two phases marked with double-headed arrows cannot run concurrently due to the geometry of the diamond interchange.

(c)

Fig. 10. (*continued*).

The purpose of Model 1 is to show the necessity and benefit of Model 2′s inclusion of constraints to account for each link's turning-in flows in the progression design. The difference between these two models lies in that, for each local path $p = (\ell, m, n)$, the inflow to link ℓ in Model 2 can be from the upstream through and side-street turning-in traffic(i.e., $m \in$ {LT,TH,RT}), whereas in Model 1 inflows are only from upstream through movements (i.e., $m =$ TH), including paths p_1, p_2, p_3, as shown in Fig. 5.

For a fair comparison, these models are solved with the same set of cycle lengths and green ratios. Table 5 shows the signal plan generated with these four models, including the optimized intersection offsets and phase sequences, Table 6 shows bandwidths generated with the benchmark and the proposed models, and Table 7 summarizes the resulting MOEs, including average delay and number of stops. Fig. 11 shows the resulting progression bands for all benefited movements. Note that right-turners from intersection 3 will receive the progression during both the through and the right-turn overlapping phases.

As expected, since the control objective of TRANSYT16 is to minimize the total delay and number of stops for the entire network, the progression bands it generates are not comparable with the proposed models. This can be observed with TRANSYT's average bandwidth of 78.6(sec) per intersection comparing to those ranging from 90.4 to 124.6 (sec) with progression methods.

Parts of the differences between the bandwidths produced by Multiband and the proposed model (in Table 6) can be attributed to their discrepancy in defining the progression bands. Note that

(i) The progression bands produced by Multiband are symmetric to the centerlines, while the proposed model does not require the bands to follow a centerline between intersections, thus allowing the band searching to be more flexible and best use the available green time. For example, Multiband reports a through bandwidth of 103 (sec) for link 4 ($l4, p_1$), but the proposed model can produce an asymmetric band of 125 (sec).

(ii) The bandwidths produced from the proposed models exclude the queue clearance times at the onset of a green phase (Little et al., 1981) because vehicles arriving during such a time window will actually encounter the initial queues rather than progressing through the intersection. In contrast, Multiband considers such queue clearance time as a portion of their produced

Table 3
Numerical Values and the Derivation of Input Parameters.

Parameter	Numerical value	Derivation
$L_{\ell,\mathrm{LT}}$	Listed in Fig. 10 (a)	From satellite images.
$N_{\ell,n}$	Listed in Fig. 10 (a)	From satellite images.
$q_{\ell,m}$ and$q_{\ell,m}$	Listed in Fig. 10 (b)	From intersection turning volume counts
c	180 (sec)	From the critical lane volume method (Webster, 1958; Messer and Fambro, 1977; Ackleik, 1981; MDOT SHA, n.d.)
$\phi_{\ell,n}$	Listed in Fig. 10 (c)	From the critical lane volume method (Webster, 1958; Messer and Fambro, 1977; Ackleik, 1981; MDOT SHA, n.d.)
$s_{\ell,\mathrm{TH}}$	2000 (veh/h)	Referenced to field data. If with a shared lane, apply volume-weighted values with turning movement counterparts.
$s_{\ell,\mathrm{LT}}$	1833 (veh/h)	Referenced to field data.
$s_{\ell,\mathrm{RT}}$	1666 (veh/h)	Referenced to field data.
ρ^{I}	0.042 (veh/ft)	From the satellite image.
T_p	Link-dependent	Ratio of link length (Fig. 10(a)) over progression speed, which is assumed to be posted speed limit. Turning vehicles are further added with 5(sec) of progression time to take into account their slower speed with turning maneuver.
$T^{B}_{\ell,\bar{n}\to n}$	Link-dependent	Ratio of bay length (Fig. 10(a)) over progression speed, which is assumed to be posted speed limit.
I	5 (sec)	specify with the reference from the state of the practice in Maryland.

Table 4
Volume calibration under the scenario with various path volumes.

Link	Major Path(s) Passing the Link	Field data (veh/h)	Simulated Volume (GEH statics)[a] (veh/h)			
			Baseline	Moderate Path Flow	High Path Flow	Heavy Path Flow
$l1$	Path A	1788	1774.6 (0.32)	1779 (0.21)	1783(0.12)	1778(0.24)
$l5$	Path A	2093	2070.6 (0.49)	2078 (0.32)	2070(0.50)	2045(1.06)
$l6$	Paths B, D	2793	2731.8 (1.16)	2753 (0.77)	2749(0.84)	2710(1.58)
$l10$	Paths B, C	3195	3114.8 (1.43)	3124 (1.27)	3154(0.73)	3092(1.83)

Note: [a] GEH statics smaller than 5.0 are considered qualified from FHWA guidelines (Dowling et al., 2004).

Table 5
Signal plans generated by the benchmark and the proposed models.

		TRANSYT[c]		Multiband		Model 1		Model 2	
Offset[a] (sec)	Intersection 1	0		0		0		0	
	Intersection 2	143		80		163		163	
	Intersection 3	12		83		141		164	
	Intersection 4	59		69		118		135	
	Intersection 5	96		51		120		138	
	Intersection 6	91		173		139		152	
Phase Sequence[b]		Arterial	Crossing Street[d]	Arterial	Crossing street[d, e]	Arterial	Crossing street[d]	Arterial	Crossing street[d]
	Intersection 1	Lead-lag	EB → WB	Lag-lead	EB → WB	Lead-lag	WB→EB	Lead-lag	EB→WB
	Intersection 2	Lead	WB → EB	Lead-lag	WB → EB	Lead	WB→EB	Lead	WB→EB
	Intersection 3	Lead	WB→EB	Lead-lag	WB→EB	Lead	WB→EB	Lead	WB→EB
	Intersection 4	Lead	N/A	Lag	N/A	Lead	N/A	Lead	N/A
	Intersection 5	Lead	N/A	Lead	N/A	Lead	N/A	Lead	N/A
	Intersection 6	Lead-lag	WB → EB	Lead-lag	WB → EB	Lag-lead	WB→EB	Lag-lead	EB→WB

Notes: LT = left turn; EB = eastbound; WB = westbound;
[a] Offsets are referenced to intersection 1.
[b] Lead = leading left-turn phase; Lag = lagging left-turn phase; Lead-lag = southbound left-turn with leading phase whereas northbound left-turn with lagging phase; Lag-lead = southbound left-turn with lagging phase whereas northbound left-turn with leading phase.
[c] Split is fixed in TRANSYT for a fair comparison.
[d] EB → WB indicates that eastbound traffic proceeds ahead of the westbound traffic and vice versa
[e] The phase sequence of the side streets is fixed in Multiband

bandwidths. As such, Multiband can yield the through bandwidth of 55 (sec) for link 5 ($l5, p_1$), but only 23 (sec) from the proposed model.

In addition, other parts of the resulting differences can be attributed to the proposed model's embedded formulations to specifically minimize potential mutual blockages between different traffic streams. For example, although Multiband generates 59 (sec) of through bandwidth for link 3 ($l3, p_1$), it would be viewed as having zero effective bandwidth in practice, because the overflows from left-turn queues actually block the through lanes over the entire through phase. In other words, since Multiband does not consider the impact of the left-turn queue, the phase sequence it produces may allow wide through bandwidths with lagging left-turn phases, which is prone to cause left-turn queue overflow. To mitigate such undesirable traffic patterns, the proposed model has reduced the number of lagging left-turn phases from five to two for the entire arterial, as shown in Table 5.

The contributions of the proposed model can be viewed from the results in the following two aspects:

A. *Improved Network Performances*

As shown in Table 7, Model 2, compared to Multiband, can effectively improve the network's overall performances by 5.8% in the network-wide average delay and 9.9% in the number of stops, whereas Model 1 yields a less reduction of 3.9% and 8.9%, respectively. The improvement with the proposed model with respect to the through traffic flows traversing the entire arterial is more significant, exhibiting about a 21.0% reduction in the number of stops over the entire arterial. This is due to the fact that the offsets and phase sequences in the proposed model are formulated to minimize the impacts from the turning-bay spillback or blockage. Such improvements for the through movements may in turn contribute to the delay reduction for the arterial's turning volumes since the left-turn bay blockages are less likely to occur. Reductions of 6.5% in the delays and 26.8% in the number of stops for all turning movements from the arterial, as shown in the third set of data in Table 7, further confirm such contributions.

Table 6
Bandwidths of local paths and connected paths.

		Bandwidth				Effective Bandwidth			
		T16 [a]	Multiband [b]	Model 1	Model 2	T16 [a]	Multiband [b]	Model 1	Model 2
Local Progression Bands									
Through									
$(\nearrow 1, p_1)$	[1SBTH,2SBTH]	52	23 (24)[c]	65	65	52	23	65	65
$(\nearrow 2, p_1)$	[2SBTH,3SBTH]	0	30 (24)[c]	30	30	0	30	30	30
$(\nearrow 3, p_1)$	[3SBTH,4SBTH]	59	59 (59)[c]	48	42	59	0	33	33
$(\nearrow 4, p_1)$	[4SBTH,5SBTH]	86	125 (103)[c]	125	125	86	95	95	95
$(\mathit{l}5, p_1)$	[5SBTH,6SBTH]	0	23 (55)[c]	20	20	0	23	2	2
$(\nearrow 6, p_1)$	[6NBTH,5NBTH]	74	7 (74)[c]	74	74	74	0	65	74
$(\nearrow 7, p_1)$	[5NBTH,4NBTH]	97	82(112)[c]	99	99	97	82	99	99
$(\nearrow 8, p_1)$	[4NBTH,3NBTH]	19	70(101)[c]	89	90	19	21	88	90
$(\nearrow 9, p_1)$	[3NBTH,2NBTH]	0	32(37)[c]	43	43	0	0	43	43
$(\nearrow 10, p_1)$	[2NBTH,1NBTH]	6	0(37)[c]	33	33	1	0	24	24
Turning-out									
$(\nearrow 8, p_2)$	[4NBTH,3NBLT]	0	21	20	26	0	0	20	26
$(\nearrow 9, p_2)$	[3NBTH,2NBLT]	0	12	0	0	0	0	0	0
$(\nearrow 10, p_2)$	[2NBTH,1NBLT]	6	14	24	24	0	0	24	24
Turning-in									
$(\nearrow 1, p_7)$	[1EBRT,2SBTH]	19	0	0	0	19	0	0	0
$(\nearrow 1, p_4)$	[1WBLT,2SBTH]	13	0	0	0	0	0	0	0
$(\nearrow 2, p_7)$	[2EBRT,3SBTH]	15	0	0	0	15	0	0	0
$(\nearrow 3, p_7)$	[3EBRT,4SBTH]	31	51	69	73	11	0	69(0)[d]	73
$(\nearrow 5, p_7)$	[5EBRT,6SBTH]	17	0	0	0	13	0	0	0
$(\nearrow 6, p_4)$	[6EBLT,5NBTH]	5	0	0	0	0	0	0	0
$(\nearrow 7, p_4)$	[5EBLT,4NBTH]	7	0	0	0	7	0	0	0
$(\nearrow 9, p_5)$	[3EBLT,2NBLT]	0	0	0	12	0	0	0	0
$(\nearrow 10, p_4)$	[2EBLT,1NBTH]	14	24	0	0	14	24	0	0
$(\nearrow 10, p_5)$	[2EBLT,1NBLT]	9	0	0	0	9	0	0	0
Avg. bandwidth									
Through		**78.6**	**90.4 (125.2)**[c]	**125.2**	**124.6**	**77.6**	**54.8**	**108.8**	**110.8**
Turning-out		**1.2**	**9.2**	**8.8**	**9.8**	**0.0**	**0.0**	**8.8**	**9.8**
Turning-in		**26.0**	**15.0**	**13.8**	**17.0**	**17.6**	**4.8**	**13.8**	**14.7**
All Paths		**105.8**	**114.7**	**147.8**	**151.3**	**95.2**	**59.6**	**131.4**	**135.3**
% Through Band Effective						98.7%	60.6%	86.9%	89.0%
% Turning Band Effective						64.7%	19.8%	88.2%	91.3%
Connection Bands									
Along arterial									
$(\nearrow 1, p_1)$	[1SBTH,2SBTH,3SBTH]	0	11	30	30	0	11	30	30
$(\nearrow 2, p_1)$	[2SBTH,3SBTH,4SBTH]	0	30	20	14	0	0	20	4
$(\nearrow 3, p_1)$	[3SBTH,4SBTH,5SBTH]	32	59	47	42	32	59	47	33
$(\nearrow 4, p_1)$	[4SBTH,5SBTH,6SBTH]	0	23	20	20	0	23	2	2
$(\nearrow 6, p_1)$	[6NBTH,5NBTH,4NBTH]	40	7	74	74	40	0	74	74
$(\nearrow 7, p_1)$	[5NBTH,4NBTH,3NBTH]	4	70	76	82	4	21	76	82
$(\nearrow 8, p_1)$	[4NBTH,3NBTH,2NBTH]	0	32	43	43	0	0	43	43
$(\nearrow 9, p_1)$	[3NBTH,2NBTH,1NBTH]	0	0	33	33	0	0	24	24
Turning-in									
$(\nearrow 2, p_7, p_1)$	[2EBRT,3SBTH,4SBTH]	15	0	0	0	15	0	0	0
$(\nearrow 3, p_4, p_1)$	[3WBLT,4SBTH,5SBTH]	13	0	13	0	13	0	0	0
$(\nearrow 3, p_7, p_1)$	[3EBRT,4SBTH,5SBTH]	31	30	53	73	11	0	48(0)[d]	60
$(\nearrow, 7 p_4, p_1)$	[5EBLT,4NBTH,3NBTH]	6	0	0	0	6	0	0	0
Turning-out									
$(\nearrow 7, p_1, p_2)$	[5NBTH,4NBTH,3NBLT]	0	21	7	13	0	0	7	13
$(\nearrow 8, p_1, p_2)$	[4NBTH,3NBTH,2NBLT]	0	12	0	0	0	0	0	0
$(\nearrow 9, p_1, p_2)$	[3NBTH,2NBTH,1NBLT]	0	14	24	24	0	0	24	24
Avg. Connection Bandwidth									
Through		**19.0**	**58.2**	**85.9**	**84.5**	**19.0**	**28.4**	**78.8**	**72.7**
Turning-in		**16.3**	**7.6**	**16.5**	**18.4**	**11.3**	**0.0**	**12.0**	**15.7**
Turning-out		**0.0**	**11.6**	**7.6**	**9.1**	**0.0**	**0.0**	**7.6**	**9.1**
All Paths		**35.3**	**77.3**	**110.0**	**112.0**	**30.3**	**28.4**	**98.5**	**97.5**

(*continued on next page*)

Table 6 (*continued*)

	Bandwidth				Effective Bandwidth			
	T16 [a]	Multiband [b]	Model 1	Model 2	T16 [a]	Multiband [b]	Model 1	Model 2
% Through Band Effective					100.0%	48.7%	91.8%	86.0%
% Turning Band Effective					69.3%	0.0%	81.4%	90.3%

Notes:
[a] T16 = TRANSYT 16. TRANSYT16 does not generate bandwidths directly, but one can apply the proposed Model 2 to evaluate bandwidths on the same computation basis. By firstly computing the optimized signal plan from TRANSYT16, one can then run Model 2 with the fixed signal plan generated from TRANSYT to obtain the bandwidths.
[b] Multiband does not generate bandwidths for turning-in and turning-out flows; hence, its turning bandwidths are generated by firstly optimizing the signal plan with Multiband; and then providing such signal plans for Model 2 to produce the bandwidths for all path flows
[c] Values in parenthesis are the bandwidths reported by Multiband.
[d] Values in parenthesis are not explicitly reported by Model 1 due to the lack of modeling turning-in flows.

Table 7
MOEs from the simulation experiments.

	Average delay (s/veh)				Average # of stops (-/veh)			
	TRANSYT	Multiband	Model 1	Model 2	TRANSYT	Multiband	Model 1	Model 2
Network [a]	**164.2**	**145.5**	**139.8** (−3.9%)[b,c]**	**137.1** (−5.8%)[b,c]***	**3.16**	**3.13**	**2.85** (−8.9%)[b,c]***	**2.82** (−9.9%)[b,c]***
Standard Deviation	12.3	13.0	13.2 (1.02)[d]	11.9 (1.27)[d]	0.19	0.21	0.19 (0.022)[d]	0.22 (0.023)[d]
Through on the Arterial[e]	**272.9**	**214.7**	**196.7** (−8.4%)[b,c]***	**190.5** (−11.3%)[b,c]***	**4.74**	**4.38**	**3.49** (−20.3%)[b,c]***	**3.46** (−21.0%)[b,c]***
Standard Deviation	30.0	22.5	25.9 (2.67)[d]	27.0 (2.91)[d]	0.34	0.28	0.39 (0.062)[d]	0.39 (0.068)[d]
SB	263.1	168.6	94.0	166.4	4.26	3.31	1.71	3.55
NB	278.9	243.4	226.4	205.9	5.04	5.05	3.57	3.39
Turning-out Traffic Streams from Arterial	**213.3**	**198.6**	**181.4** (−8.7%)[b,c]**	**185.8** (−6.5%)[b,c]*	**3.84**	**4.00**	**2.94** (−26.5%)[b,c]***	**2.93** (−26.8%)[b,c]***
Standard Deviation	30.02	28.13	27.3 (3.12)[d]	29.39 (3.91)[d]	0.34	0.33	0.38 (0.065)[d]	0.36 (0.077)[d]
SB to crossing streets	131.1	101.9	94.0	91.6	2.37	2.24	1.71	1.92
NB to crossing streets	254.9	249.8	226.3	232.8	4.58	4.93	3.57	3.44
Turning-in Streams from Crossing Streets[f]	184.79	151.4	161.2 (+6.5%)**	143.7 (−5.08)[b,c]***	3.69	3.35	3.67 (+9.5%)[b,c]***	3.48 (+3.8%)[b,c]**
Standard Deviation	2.57	2.47	4.24	2.99	0.08	0.10	0.09	0.06
From Democracy Rd. EB	158.4	157.5	156.4	148.2	4.60	4.24	4.61	4.47
LT from I-495 EB ramp	211.5	258.2	264.8	229.5	3.26	4.55	4.98	4.28
RT from I-495 WB ramp	134.4	147.1	124.3	118.0	3.34	3.85	3.64	3.24

Notes: LT = left turn; RT = right turn; ***= significance level of 0.001; **= significance level of 0.01; *= significance level of 0.05; ns = not significant at level of 0.05.
[a] Network-wide MOEs (delay and number of stops) are the averages of all traffic streams in and moving out of the network, including those leaving the network immediately via unsignalized right-turn movements.
[b] Compared to the MOE generated by Multiband. Paired-*t* test is applied when evaluating significance in differences.
[c] Applying paired *t*-test as the variance reduction technique. Samples are paired by the same random seed.
[d] Standard error of the paired difference.
[e] Vehicles travel along the entire arterial are sampled.
[f] Vehicles from side street and traveling along the until the north or south boundary of the network are sampled.

B. *Optimal Crossing Streets' Performances*

As shown in Table 7, Model 2 has reduced the delay per vehicle for turning-in traffic, with an average of 143.7(sec) compared to 151.4(sec) from Multiband. Notably, the average delay of such vehicles increases to 161.2(sec) in Model 1 since they are not explicitly taken into account in the progression design. Such results justify for inclusion the turning-in flows explicitly in the design of a multi-path progression system. To evaluate such improvement with simulations, the last category of results in Table 7 shows the models' performance with respect to the arterial's turning-in flows from the crossing streets. As expected, Model 2, with its function to provide progression to turning-in vehicles from side streets, can reduce the average delay and number of stops at those intersections experiencing high turning-in volumes from the crossing streets. For example, Model 2 yields an average delay of 148.2 s for eastbound traffic

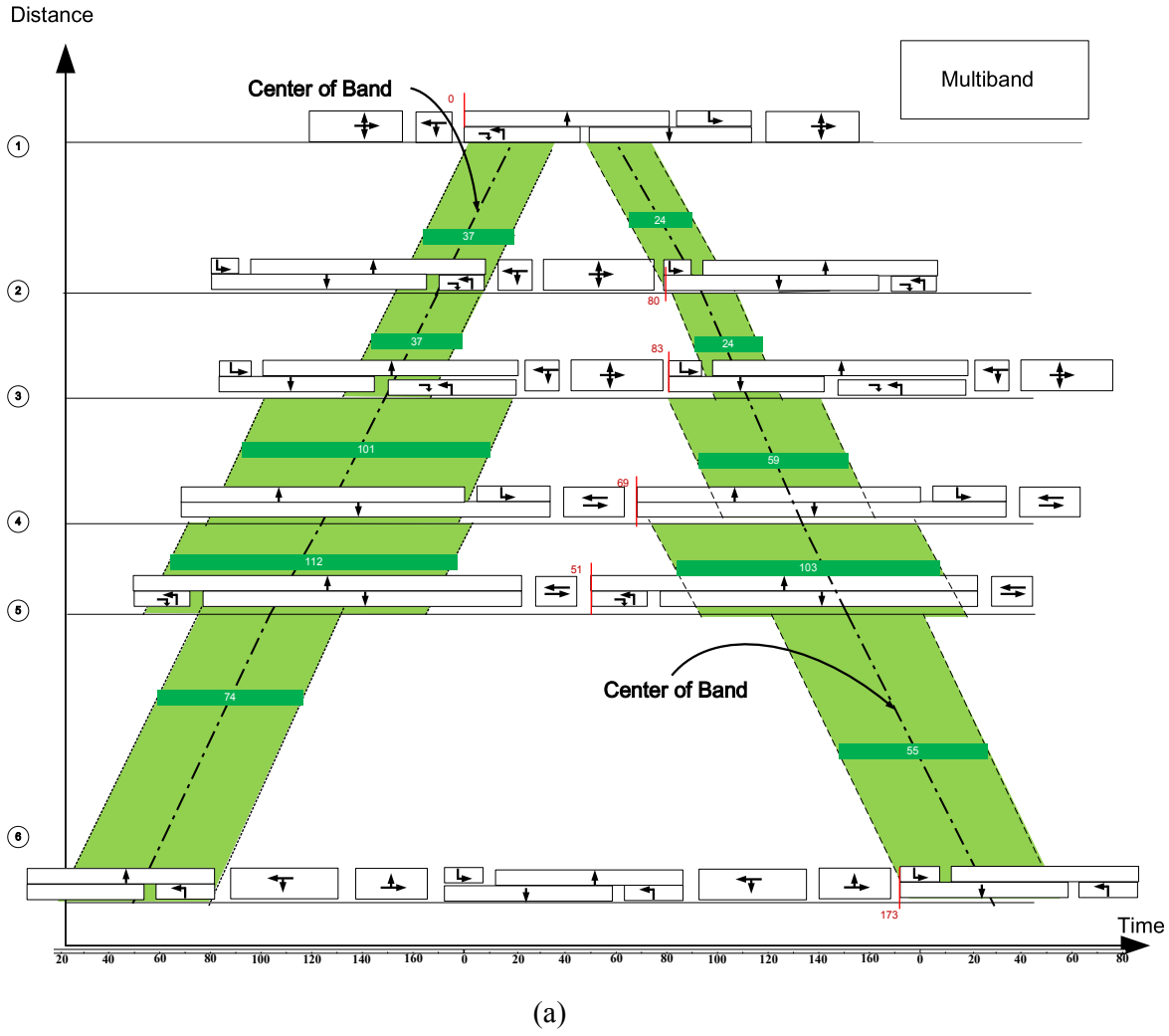

(a)

Fig. 11. Time-space diagram generated with (a) Multiband (b) Model 1 (c) Model 2 under demand scenario of field data (level-1).

from Democracy Rd, while Model 1, yielding 156.4 s of delay, exhibits only comparable performance with Multiband (157.5 s), because both do not account for those turning-in volumes in the design of progression bands.

The advantages of taking turning-in paths and flows in the multi-path arterial progression design include:

- Turning-in volumes with their designated progression bands produced from Model 2 s generally experience less average delay, as evidenced in the reduction of such delay from 161.2 to 143.7 (sec/veh), compared to Model 1;
- Providing signal progression to turning-in streams can minimize the likelihood of their incurring mutual blockages with other vehicle movements;
- Efficiently progressing turn-in traffic through a link's downstream intersection will naturally result in less traffic queues for both its through and turning-out movements, which in turn will reduce the likelihood of overflows from the turning bay and mutual blockage between turning and through traffic flows.

Some observations are worth noting:

A. *Trade-offs Between Turning-in and Turning-out Flows*

Note that by including the turn-in traffic streams, Model 2 needs to design the progression for all candidate path flows over the entire link, and best allocated the green times for progression of all movements, which, by nature, are in competition of the available bandwidth. As such, Model 2, designed with the objective to produce the maximal total weighted bandwidths, may yield the overall

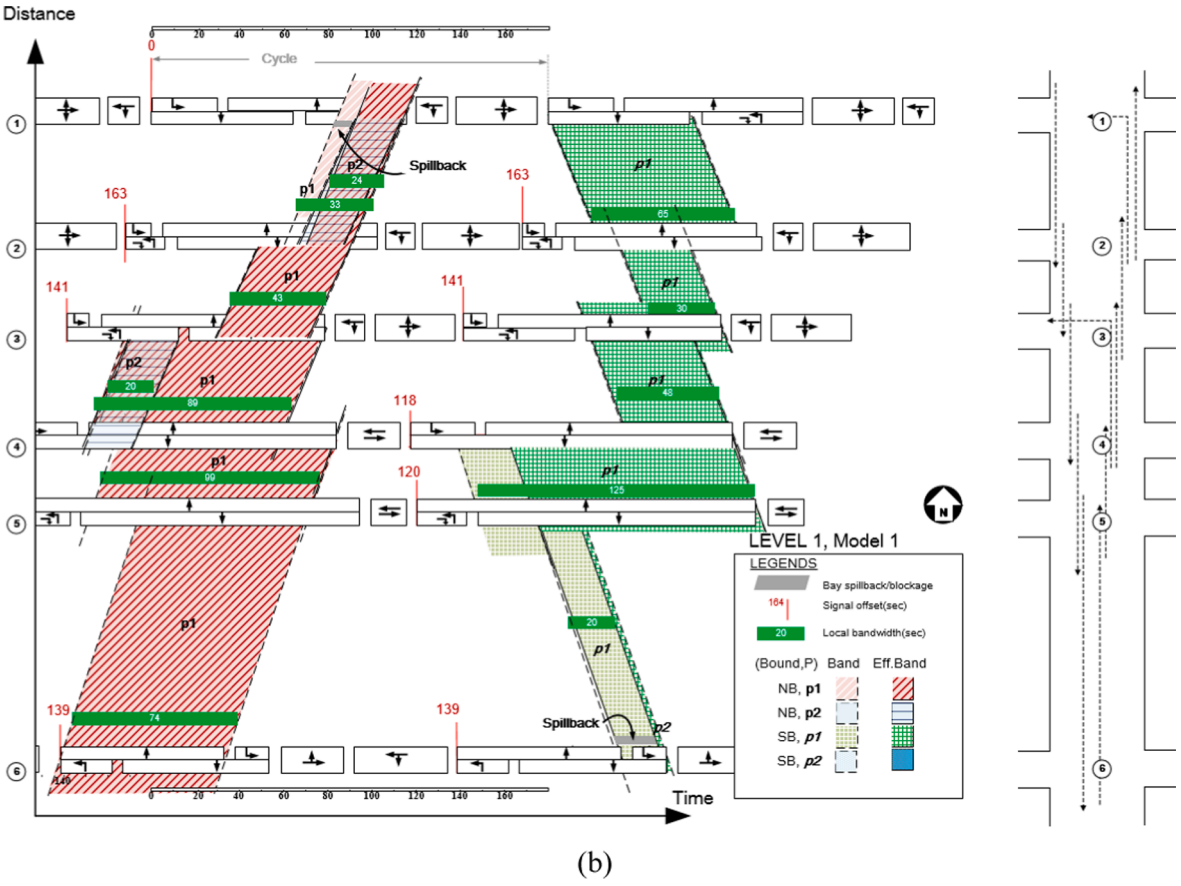

(b)

Fig. 11. (*continued*).

optimal control state that offers effective progression bands for most path flows but at the expense of some movements of less volume or having a high likelihood of impeding other traffic streams. For example, Model 2 yields a higher delay for the turning-out volumes than Model 1 (185.8 sec vs. 181.4 sec). However, such expenses are outweighed by the benefit of taking all paths into account, evidenced by the lower network delay of 137.1 sec with Model 2 compared to 139.8 sec with Model 1.

B. *Reduced Delay at Expenses of Number of Stops*

Although the average delay of turning-in traffic has decreased with Model 2, such improvement is partially at the expense of an increased average number of stops, i.e., by 3.8% compared to Multiband. This is due likely to that under the proposed system of offline in nature, all vehicles in different path-flows are assumed to behave consistently and uniformly within the assigned bandwidth to reach the downstream intersection when the queue of its own paths (initial queue) or blockage from other paths have been dissipated. However, the random nature of traffic dynamics in reality, as replicated in the stochastic microscopic simulation, may reflect the likelihood that some path-flow vehicles in their designed progression band during some intervals have to experience unexpected stops because of encountering excessive queue dissipation time due to the behavioral discrepancies of the simulated driving populations.

3.2. *Experiment 2: performance comparison with state-of-the-art using the full O-D information*

The purpose of this experiment is to show that the proposed model, circumventing the need to use the rarely available arterial O-D volume distributions, can yield comparable performance. Hence, in this experiment, the proposed model will be compared to a state-of-the-art path-based signal progression model under various path flow patterns but sharing the same set of intersection turning counts. To achieve such comparison, two other paths (See Paths C and D in Fig. 12) and their respective volumes are identified in addition to two-way through movements along the arterial.

As shown in Table 8, three scenarios with moderate, high, and heavy path flows are generated in addition to the baseline scenario. All these scenarios share the same set of intersection turning counts, but the volumes for those given traffic moving paths are calculated with the available intersection turning information shown in Fig. 10(b).

In experiment 2 for comparing the model performance under different path volumes, the traffic path settings must satisfy (i) the

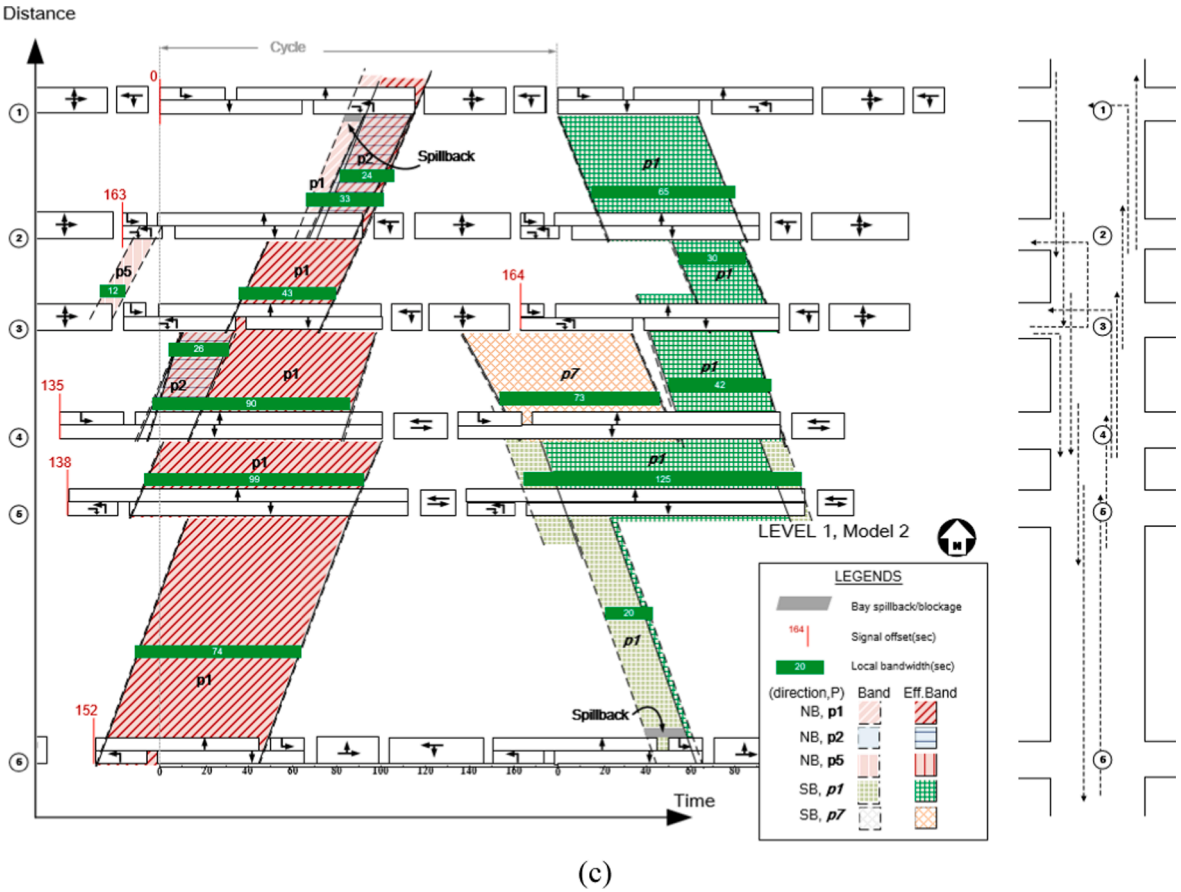

(c)

Fig. 11. (*continued*).

volumes of paths A, B, C, and D, and (ii) turning volume counts. Therefore, the volumes of paths A, B, C, and D have first been set in VISSIM for the entire route from the origin to destination. Then, the remaining volume at the intersection level will follow another set of route choice patterns, also specified in VISSIM, to satisfy the turning volume counts.

Notably, since cycle length and green splits are determined by intersection turning volume counts, and geometric conditions (Webster, 1958; Messer and Fambro, 1977; Akcelik, 1981; MDOT SHA, n.d.), the same inputs in Fig. 10(c) are applied to all scenarios in experiment 2.

For those three levels of path flow rate, the proposed model expectedly generates the identical signal settings to those in Table 5 since only turning volume counts are used in the proposed model. Fig. 12 shows the progression bands for all such levels with the Multipath model in Yang et al. (2015), and Table 9 summarizes their resulting MOEs.

In this experiment, only Multipath (Yang et al., 2015) are assumed to the full information of all path-volumes while all other models apply only intersection turning volume counts. As such, Multipath is able to provide progression for Paths C and D, but other models cannot generate comparable bandwidths.

It is noticeable from the simulation results shown in Table 9, the proposed model's performances in terms of average delay and the number of stops under these experimental scenarios at the network level are comparable to the Multipath model, i.e., different within the range of 4–7%.

The performance with respect to each path of traffic stream, however, varies with the interference level between different path flows and their volumes in different traffic scenarios. More specifically, Multipath model tends to yield better performance for those routes unlikely to experience traffic queue blockage, but the proposed model with its embedded features clearly can offer better progression for traffic on those paths that suffer inevitably from the partial mutual blockage between heavy turning and through traffic queues. Some interesting results are summarized below:

- For Path-C traffic stream that is free from potential mutual blockage, Multipath is observed to yield better MOEs than the proposed model under all such experimental scenarios. For example, the delay with the proposed model increased by 22.2% than the Multipath model under moderate path flow. Such results show the limitation of the proposed model that not all major path flows would be guaranteed to have their designated progression bands under the objective of maximizing the total bandwidth, compared to those models conditioned on the availability of complete path-volume information.

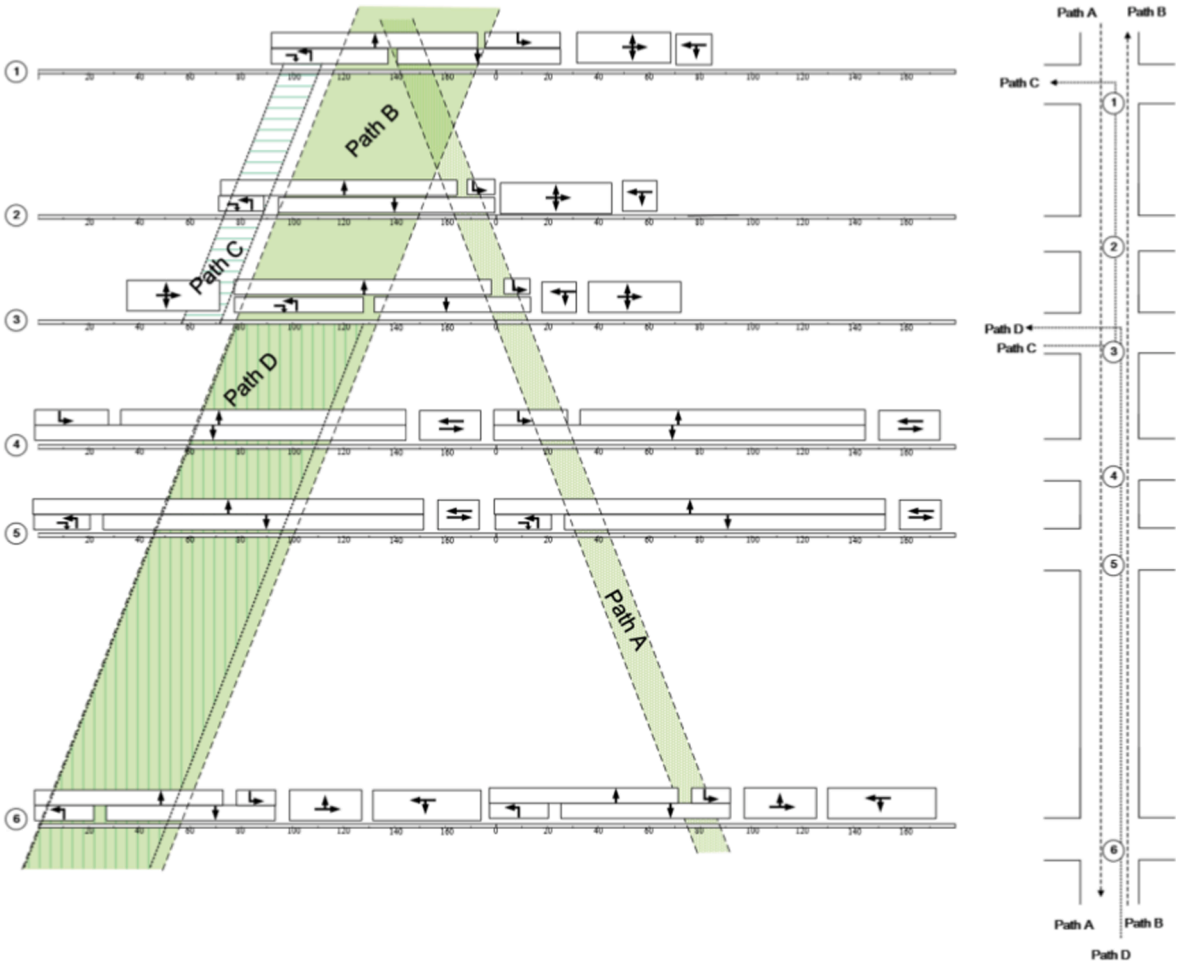

Fig. 12. Time-space diagram generated by the Yang et al. (2015)'s Multipath.

Table 8
Scenario with Various Levels of Path Flows.

Movements[a]		**Path C** 3EBLT-2NBTH-1NBLT[a]	**Path D** 6NBTH-5NBTH-4NBTH-3NBLT[a]
		Path flow rate (veh/h)	
Scenario	Baseline	100	495
	Moderate Path Flow	200	595
	High Path Flow	300	695
	Heavy Path Flow	400	729

Notes: EB = Eastbound; NB = Northbound; TH = through; LT = Left-turn
[a] Each path is expressed with a set of intersection numbers followed by the turning movements.

- For vehicles along Path-D, which may experience only a moderate level of interferences by traffic queues or bay overflows, both models yield a comparable level of average delay, but the proposed model generates a much fewer number of stops (10–16% improvement).
- For vehicles taking Path A or Path B under these three experimental scenarios, they are doomed to encounter some blockages by either overflows from the turning bay or excessive through or turning queues. As such, the proposed model with its embedded feature to circumvent such impedances can yield much better MOEs than the path-based model under these experimental traffic scenarios.
- Although the proposed model has included all major path flows in the design of a multi-path progression plan, under the objective of maximizing the total bandwidth for all path flows and the constraints of available green duration and geometric features, some paths of relatively low volumes may not receive their designated progression bands.

Table 9
Comparison of MOEs with proposed model using only turning volume counts and Multipath in Yang et al. (2015) using the arterial O-D information.

		Delay (s/veh)				# Stops (-/veh)			
		Multiband	**Multipath** in Yang et al. (2015)	**Proposed**	**Percent Change**[c]	**Multiband**	**Multipath** in Yang et al. (2015)	**Proposed**	**Percent Change**
Moderate Path Flow	**Network Overall**	**146.2** (14.5)[a]	**148.5** (10.8)[a]	**140.8** (16.4)[a]	**−5.2%*** (2.52)[b]	**3.11** (0.24)[a]	**3.17** (0.16)[a]	**2.94** (0.28)[a]	**−7.3%***** (0.062)[b]
	Path A	162.1	241.1	162.8	−32.5%	3.12	5.21	3.46	−33.6%
	Path B	251.0	228.2	212.5	−6.9%	5.07	4.00	3.63	−9.3%
	Path C	206.2	181.3	221.6	22.2%	5.15	3.74	6.41	71.4%
	Path D	225.7	231.3	230.1	−0.5%	4.47	3.88	3.36	−13.4%
High Path Flow	**Network Overall**	**147.2** (12.1)[a]	**146.7** (12.8)[a]	**140.4** (12.1)[a]	**−4.3% *** (2.49)[b]	**3.11** (0.16)[a]	**3.17** (0.20)[a]	**2.93** (0.17)[a]	**−7.6%**** (0.070)[b]
	Path A	154.5	236.1	164.9	−30.1%	2.90	5.08	3.56	−29.9%
	Path B	262.1	216.6	207.7	−4.1%	4.93	3.67	3.45	−6.0%
	Path C	238.9	199.0	232.2	16.7%	6.12	5.65	6.73	19.1%
	Path D	221.6	227.5	226.5	−0.4%	4.30	3.66	3.05	−16.7%
Heavy Path Flow	**Network Overall**	**147.9** (15.5)[a]	**151.7** (14.5)[a]	**145.7** (16.8)[a]	**−4.0%,** ns (11.3)[b]	**3.31** (0.38)[a]	**3.58** (0.49)[a]	**3.41** (0.56)[a]	**−4.7%,** ns (0.44)[b]
	Path A	162.8	232.3	163.2	−29.8%	3.21	5.04	3.47	−31.2%
	Path B	246.7	218.2	202.7	−7.1%	4.83	3.73	3.40	−8.8%
	Path C	259.4	245.3	276.0	12.5%	6.93	8.10	9.41	16.2%
	Path D	215.1	222.0	223.4	0.6%	4.16	3.51	3.16	−10.0%

Notes: ***= significance level of 0.001; **= significance level of 0.01; *= significance level of 0.05; ns = not statically different at significant level of 0.05.
[a] Standard Deviation;
[b] Standard Error of paired difference by pairing random seed as a variance reduction technique.
[c] Comparing the proposed model with Multipath

3.3. *Experiment 3: evaluating the benefits of accounting for turn-in volumes and variable phase sequence in the design*

The third set of experiments, comprising the following four levels of volume scenarios, is designed to show that involving variable phase sequence plans and turning volumes from side streets into the arterial signal design can yield a more effective control plan for the entire arterial flows.

- Level-1: the field data with very high turning flows. As shown in Fig. 10(b), the left-turn volume on the arterial can be up to 729 vph at intersection 3, and the turning-in volumes from the crossing street are at the level of up to 677 vph, at intersection 2;
- Level-2: reduce the volume from Level-1 scenario by 100 vph for each turning movement if its volume is larger than 200 vph.
- Level-3: further reduce the volume from Level-2 scenario by 100 vph for each turning movement if its volume is larger than 200 vph.
- Level-4: generate a scenario of low turning-volume ratios by reducing the volume from Level-3 by 100 vph for each turning movement if its volume is larger than 200 vph.

All these four scenarios will be solved by the proposed model, and the MOEs for comparison include the average local through bandwidths, average effective through bandwidths, average connection bandwidths, and average effective connection bandwidths for

Table 10
Numerical results from experiment 3.

	Average Through Bandwidth (s)		Average Connection Bandwidth (s)	
	Fixed Sequence	Var[a] Sequence	Fixed Sequence	Var[a] Sequence
Level 1 (Field)	114.1 (106.3)[b]	124.6 (110.8)[b]	97.4 (87.9)[c]	112.0 (97.5)[c]
Level 2	132.4 (120.6)[b]	137.8 (123.3)[b]	123.4 (111.3)[c]	131.6 (116.4)[c]
Level 3	144.5 (127.4)[b]	150.8 (126.2)[b]	136.7 (121.5)[c]	140.4 (120.6)[c]
Level 4	151.2 (133.2)[b]	157.9 (126.2)[b]	145.4 (123.3)[c]	150.4 (119.9)[c]

Notes:
[a] Var. = Variable.
[b] Values shown in parenthesis are the average effective through bandwidth not impacted by spillback.
[c] Values shown in parenthesis are the average effective connection bandwidth not impacted by spillback.

multi-intersection progression. The MILP is solved with Gurobi 9 and the computation times are less than 316.49 s for all scenarios. The time–space diagrams of the signal plans obtained from the Level-1 and Level-3 scenarios are shown in Fig. 11(c) and Fig. 13, respectively.

A. Turning Volumes may Affect the Through Bandwidths

The comparison results with different turning volumes in Table 10 show that the local through bandwidth will increase with a decrease in turning volumes, so is the average connection bandwidth for multi-intersection progression, defined in Eqs. (21)–(22). The relation that reducing the turning volumes will increase the optimal bandwidth for through movements can also be observed from Fig. 11(c) and Fig. 13, where the bandwidths for through movements are significantly wider under lower left-turn volumes, as, for example, shown in the local path between intersections 2 and 3 ($l2, p_1$) (30 s and 52 s under Level-1 and Level-3, respectively). It is also evidenced that the smaller through bandwidths in Level-1 allow the wider bandwidths for turning movements. For example, one can clearly observe a wider turning bandwidth for the northbound left-turn movement at intersection 3 from intersection 4 ($l8, p_2$) if comparing the results in Fig. 11(c) and with that in Fig. 13 (i.e., 26 and 10 s under Level-1 and Level-3, respectively).

B. Necessity of Incorporating the Impacts from the Potential Spillbacks in Signal Design

Table 10 shows the comparisons of the local bands and their effective portions, indicating that the proposed model under a high turning volume scenario is capable of reducing the potential interference from the queues with the following embedded logic:

- Circumventing the left-turn queue spillback completely and providing through progression with the optimized offsets and variable phase sequences. For example, as shown in Fig. 11(c), the leading northbound left-turn phase at intersection 3 allows the left-turn queue to be fully discharged over the first 11 s of the cycle (refer to the time axis in the diagram), before the band for the northbound through path arrives from its upstream intersection.
- Minimizing the impacts of queue spillback (if inevitable) to the through progression with the carefully designed constraints. For example, as shown in Fig. 11(c), left-turn queues inevitably spill back in the northbound approach of intersection 1, based on its

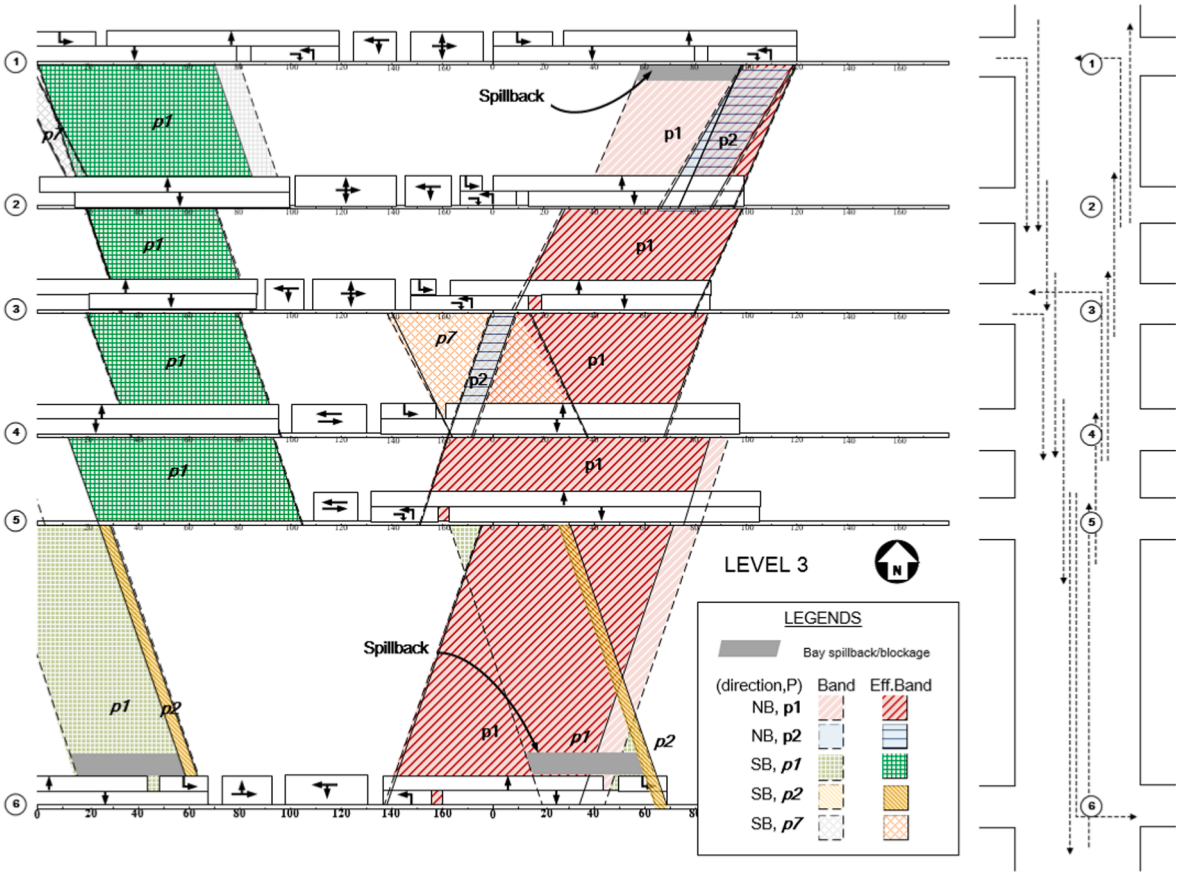

Fig. 13. Time-space diagram generated with the proposed model under demand scenario level-3.

high volume, green duration, and limited bay length, but by synchronizing the left-turn green phase with the band for the local through path, its impact is limited to merely 10 s (from 83 to 93 s of cycle) so that the effective bandwidth can be maximized.

- Reducing the impacts of long through queues on the left-turn movements. For example, as shown in Fig. 11(c) and Fig. 13, the path flows taking the northbound left-turn at intersection 3 have received their progression bands at 11 s of the cycle while the through queue already vanishes, so the blockage to left-turners can be averted.

In summary, capturing the interrelations between queue formation and vehicles in the progression band provides critical information for best design the signal progression. Preventing the impacts from left-turn queue spillback on the through paths can increase their bandwidths for through vehicles, which will in turn reduce queues by through vehicles and their impacts on left-turning flows. Hence, the mutual blockage between left-turn and through queues can be minimized with the optimized offsets and variable phase sequences for all local path flows.

C. Generating a Wider Band with Variable Phase Sequences

The comparison between fixed and variable phase sequences in Table 10 shows that the average bandwidths, under all tested scenarios, can be further improved with the variable and optimized phase sequences. For example, the average through bandwidth increased from 114.1 to 124.6(sec) under variable phase sequences at the Level-1 demand, and their corresponding effective through bandwidth, not impeded by spillbacks, also increased from 106.3 to 110.8(sec).

In summary, the results from numerical experiments with different turning volumes confirm that the proposed model is capable of: 1) distributing a longer green time to progress the turning movements of higher volume; 2) identifying and minimizing the impacts of mutual blockages between the queues from through and left-turn movements, and 3) optimizing the phase sequences to increase the progression efficiency.

4. Conclusions

Congested urban arterials, connecting multiple major intersections with both heavy turning and through flows, often cannot yield the expected level of performance even under the objective of maximizing two-way signal progression, due mainly to the potential mutual blockage between the through vehicles and spillback flows from the turning bay. To design the signal plans for such arterials, this study has proposed a MILP model that can provide progression bands for each candidate path along the target arterial without the information of O-D or the volume of each path flow.

The proposed model aims to construct local progression bands for vehicles on all local paths and then designed the optimal connection between two local through bands for neighboring links with the optimized offsets and phase sequences under the control objective of maximizing the total weighted progression bands for the entire arterial. To ensure the effectiveness of the produced local bands for each link's connection of its upstream and downstream flows and the connected through bands for multi-link flow progression, the proposed model can exercise its embedded functions to estimate some key information associated with the design of offsets and phase sequence, including the spillback duration from a turning bay, the impeded duration within a local path's progression band due typically to mutual queue blockage, and the estimated vehicle volume within each designated progression band.

The results from the extensive simulation experiments have confirmed that the proposed model can indeed yield the expected performance with respect to the selected MOEs of the total network delay and number of stops, compared to the benchmark model, Multiband (Gartner et al., 1991). Those improvements are due to the proposed model's embedded functions to minimize the impacts from left-turn spillback on the through-path flows, as evidenced by the reduction in delay and number of stops by 11.3% and 21.0%, respectively. Allowing each intersection's tuning flows, either from its upstream through or turning movements to have designated progression bands also contribute to the improvements on all MOEs. In addition, the proposed model has also been designed with a special feature to account for the side-street volume in selecting these local paths for progression and design of optimal offsets as well as phase sequences for maximizing of the total benefit for the entire arterial.

Whether to apply the proposed models or any of the state-of-practice models should be based on the likelihood and the duration of incurring turning queue spillback. One can first apply an existing method to estimate the *distance of intersection queues* (e.g., see chapter 31 of HCM 2016) and then compare the results with the turning bay length. Notably, such estimated queue distance cannot be directly utilized for optimizing the arterial's progression design because its relation with the adopted signal plan is interdependent, and such queue distance will be minimized under the optimized phase sequence and offsets produced by the proposed model. Hence, to be conservative in practice, one can first compute the queue distances with the historical volume data under a worst-case scenario with any existing establish method, and then adopt our proposed model the likelihood of having mutual queue blockage has been identified over the target period of analysis

It should be noted that despite the emergence of various real-time traffic-responsive systems over the past decades, their effectiveness still relies on a reliable offline model as the backbone for computing the baseline control strategies. For example, the real-time network control system, SCOOT, relies on its offline version, TRANSYT models (Hunt et al., 1982), to provide the initial optimal signal plan. A vast body of studies on the progression band maximization has demonstrated the effectiveness under pre-timed control environments for decades before the adoption by SCATS for online generation of a progression-based network signal system (Sims and Finlay, 1984) Also, most adaptive traffic systems for network signals usually require a set of offline optimized parameters as the basis to activate the adaptive process (Jin and Ma, 2017). Thus, the model proposed in this study can be used not only for the design of multi-path progression for pre-timed control of congested arterials, but also be applied as the core module for their real-time operations

under actuated or responsive control.

Future extension along the line will include refinement of the connection between two local through bands so as to ensure that the bandwidth for multi-link progression will not be reduced over consecutive links. Integrating the proposed model with real-time available traffic data for contending with time-varying traffic conditions shall also be a viable extension. In addition, refining the model's formulations to account for the input data variances so as to improve the robustness of the optimized signal plan should also be one vital task for enhancing the proposed model to use in practice.

CRediT authorship contribution statement

Yen-Hsiang Chen: Conceptualization, Methodology, Validation, Writing – original draft, Writing - review & editing. **Yao Cheng:** Methodology, Writing – original draft, Writing - review & editing. **Gang-Len Chang:** Conceptualization, Writing – original draft, Writing - review & editing, Supervision.

Declaration of Competing Interest

The authors declare that they have no known competing financial interests or personal relationships that could have appeared to influence the work reported in this paper.

References

Aboudolas, K., Geroliminis, N., 2013. Perimeter and boundary flow control in multi-reservoir heterogeneous networks. Transp. Res. Part B: Methodol. 55, 265–281.

Akcelik, R., 1981. Traffic signals: capacity and timing analysis.

Arsava, T., Xie, Y., Gartner, N.H., 2016. Arterial progression optimization using OD-BAND: case study and extensions. Transp. Res. Rec. 2558 (1), 1–10.

Arsava, T., Xie, Y., Gartner, N., 2018. OD-NETBAND: an approach for origin-destination based network progression band optimization. Transp. Res. Rec. 2672 (18), 58–70.

Binning, J.C., 2019. TRANSYT 16 User Guide, TRL Limited 2019.

Chaudhary, N.A., Kovvali, V.G., Chu, C.L., Kim, J., Alam, S.M.M., 2002. Software for timing signalized arterials (No. FHWA/TX-03/4020-1,).

Chang, E.C., Cohen, S.L., Liu, C., Chaudhary, N.A., Messer, C., 1988. MAXBAND-86: Program for optimizing left-turn phase sequence in multiarterial closed networks. Transportation Research Record, (1181).

Chen, Y.H., Cheng, Y., Chang, G.L., 2019. Concurrent progression of through and turning movements for arterials experiencing heavy turning flows and bay-length constraints. Transp. Res. Rec. 2673 (9), 525–537.

Cheng, Y., Chang, G.L., Rahwanji, S., 2018. Concurrent optimization of signal progression and crossover spacing for diverging diamond interchanges. J. Transp. Eng., Part A: Syst. 144 (3), 04018001.

Christofa, E., Ampountolas, K., Skabardonis, A., 2016. Arterial traffic signal optimization: a person-based approach. Transp. Res. Part C: Emerg. Technol. 66, 27–47.

Dowling, R., Skabardonis, A., Alexiadis, V., 2004. Traffic analysis toolbox, volume III: Guidelines for applying traffic microsimulation modeling software (No. FHWA-HRT-04-040). United States. Federal Highway Administration. Office of Operations.

Gartner, N.H., Assman, S.F., Lasaga, F., Hou, D.L., 1991. A multi-band approach to arterial traffic signal optimization. Transp. Res. Part B: Methodol. 25 (1), 55–74.

Gartner, N.H., Stamatiadis, C., 2002. Arterial-based control of traffic flow in urban grid networks. Math. Comput. Modell. 35 (5–6), 657–671.

Gartner, N.H., Stamatiadis, C., 2004. Progression optimization featuring arterial-and route-based priority signal networks. J. Intell. Transp. Syst. 8 (2), 77–86.

HCM (Highway Capacity Manual) 6th Edition: A Guide for Multimodal Mobility Analysis, 2016. Transportation research board. National Academics of Sciences, Engineering, Medicine, Washington, DC.

Hunt, P.B., Robertson, D.I., Bretherton, R.D., Royle, M.C., 1982. The SCOOT on-line traffic signal optimisation technique. Traffic Eng. Control 23 (4).

Jin, J., Ma, X., 2017. A group-based traffic signal control with adaptive learning ability. Eng. Appl. Artif. Intell. 65, 282–293.

Kashani, H.R., Saridis, G.N., 1983. Intelligent control for urban traffic systems. Automatica 19 (2), 191–197.

Keyvan-Ekbatani, M., Kouvelas, A., Papamichail, I., Papageorgiou, M., 2012. Exploiting the fundamental diagram of urban networks for feedback-based gating. Transp. Res. Part B: Methodol. 46 (10), 1393–1403.

Keyvan-Ekbatani, M., Papageorgiou, M., Papamichail, I., 2013. Urban congestion gating control based on reduced operational network fundamental diagrams. Transp. Res. Part C: Emerg. Technol. 33, 74–87.

Li, J.Q., 2013. Bandwidth synchronization under progression time uncertainty. IEEE Trans. Intell. Transp. Syst. 15 (2), 749–759.

Little, J.D., 1966. The synchronization of traffic signals by mixed-integer linear programming. Oper. Res. 14 (4), 568–594.

Little, J.D., Kelson, M.D., Gartner, N.H., 1981. MAXBAND: A versatile program for setting signals on arteries and triangular networks.

Liu, Y., Chang, G.L., 2011. An arterial signal optimization model for intersections experiencing queue spillback and lane blockage. Transp. Res. Part C: Emerg. Technol. 19 (1), 130–144.

Lo, H.K., Chang, E., Chan, Y.C., 2001. Dynamic network traffic control. Transp. Res. Part A: Policy Pract. 35 (8), 721–744.

Maryland Department of Transportation State Highway Administration (MDOT SHA, n.d.) Traffic Signal Timing Guidelines and Training Manual Interim Edition, Maryland State Highway Administration, Hannover, MD, USA, undated.

Messer, C.J., Whitson, R.H., Dudek, C.L., Romano, E.J., 1973. A variable-sequence multiphase progression optimization program. Highway Res. Rec. 445 (1973), 24–33.

Messer, C.J., Fambro, D.B., 1977. Critical Lane Analysis for Intersection Design. Transportation Research Record, 644.

Morgan, J.T., Little, J.D., 1964. Synchronizing traffic signals for maximal bandwidth. Oper. Res. 12 (6), 896–912.

Papola, N., 1992. Bandwidth maximization: split and unsplit solutions. Transp. Res. Part B: Methodol. 26 (5), 341–356.

PTV, 2016. PTV VISSIM 9 User Manual, Karlsruhe, Germany.

Stevanovic, A., Martin, P.T., Stevanovic, J., 2007. VisSim-based genetic algorithm optimization of signal timings. Transp. Res. Rec. 2035 (1), 59–68.

Tian, Z., Urbanik, T., 2007. System partition technique to improve signal coordination and traffic progression. J. Transp. Eng. 133 (2), 119–128.

Robertson, D.I., 1969. TRANSYT: a traffic network study tool.

Sims, A.G., Finlay, A.B., 1984. SCATS, splits and offsets simplified (SOS). Australian Road Res. 12 (4).

Wallace, C.E., Courage, K.G., Reaves, D.P., Shoene, G.W., 1988. GW, Euler, and A. Wilbur, TRANSYT-7F User's Manual (Release 6) Technical Report, Prepared for FHWA by the Transportation Research Center, University of Florida, Gainesville, FL.

Wallace, C.E., Courage, K.G., 1982. Arterial progression-New design approach. Transp. Res. Rec. 881, 53–59.

Webster, F.V., 1958. Traffic signal settings, road research technical paper no. 39. Road Research Laboratory.

Yan, H., He, F., Lin, X., Yu, J., Li, M., Wang, Y., 2019. Network-level multiband signal coordination scheme based on vehicle trajectory data. Transp. Res. Part C: Emerg. Technol. 107, 266–286.

Yang, X., Chang, G.L., Rahwanji, S., 2014. Development of a signal optimization model for diverging diamond interchange. J. Transp. Eng. 140 (5), 04014010.

Yang, X., Cheng, Y., Chang, G.L., 2015. A multi-path progression model for synchronization of arterial traffic signals. Transp. Res. Part C: Emerg. Technol. 53, 93–111.
Yang, X., Cheng, Y., Chang, G.L., 2016. Operational analysis and signal design for asymmetric two-leg continuous-flow intersection. Transp. Res. Rec. 2553 (1), 72–81.
Yang, X., Chang, G.L., 2017. Estimation of time-varying origin-destination patterns for design of multipath progression on a signalized arterial. Transp. Res. Rec. 2667 (1), 28–38.
Yun, I., Park, B., 2006. Application of stochastic optimization method for an urban corridor. In: Proceedings of the 2006 Winter Simulation Conference. IEEE, pp. 1493–1499.
Zhang, C., Xie, Y., Gartner, N.H., Stamatiadis, C., Arsava, T., 2015. AM-band: an asymmetrical multi-band model for arterial traffic signal coordination. Transp. Res. Part C: Emerg. Technol. 58, 515–531.